RSC Advances

PAPER

View Article Online
View Journal | View Issue

Cite this: *RSC Adv.*, 2024, **14**, 30938

Design, synthesis, and high-throughput *in vitro* anti-cancer evaluation of novel 4-aminopyrazolo[3,4-*d*]pyrimidine derivatives: potential anti-cancer candidates against UO-31 renal cancer cells†

Amitananda Dash, [a] Guruswamy Vaddamanu,[b] Mohammed B. Hawsawi, [c] Mustafa S. Alluhaibi,[c] Pavana Kumari Gurijala*[a] and Naveen Mulakayala *[b]

Received 16th July 2024
Accepted 18th September 2024

DOI: 10.1039/d4ra05136j

rsc.li/rsc-advances

A novel series of 20 compounds containing 4-aminopyrazolo[3,4-*d*]pyrimidine core were synthesized, characterized and their chemical structures confirmed using spectroscopic techniques such as ^{1}H NMR, ^{13}C NMR, IR, and HRMS. The compound's growth inhibitory activities were evaluated against 60 human tumor cell lines from nine panels: leukemia, non-small cell lung cancer (NSCLC), colon, central nervous system (CNS), melanoma, ovarian, renal, prostate, and breast cancer. Among all the compounds, **11**, **12c**, **12d**, **12f**, and **12j** are active against different cancer cell lines. Between all the cell lines, compounds **12c**, **12d**, **12f**, **12j**, and **11** showed good inhibitory activity against renal cancer cell lines. From the five-dose study, based on IC_{50} values, the order of activity of compounds against renal cancer cell lines was found to be **12c** > **12f** > **12c** > **12j** > **11** with **12c** being the most potent, was better than sunitinib and sorafenib. Having been recognized as initial hits, these substances need additional pharmacological investigation.

Introduction

Cancer continues to be a significant global challenge. It was responsible for an estimated 9.7 million deaths, with approximately 20 million new cases worldwide in the year 2022.[1] The World Health Organization (WHO) has predicted a 77% increase in cancer burden globally by the year 2050.[2] Pyrimidines are a fundamental class of hetero-aromatic compounds that play a crucial role in forming essential components of DNA and RNA, such as cytosine, thymine, and uracil. Their simple yet functionalized structures make them vital scaffolds in synthesizing many drugs and biologically active compounds, including anti-cancer drugs.[3,4] Derivatives of pyrimidine moiety were known to mimic the natural pyrimidines and interfere with many important biological targets, making them a vital scaffold in the synthesis of novel anti-cancer agents.[5] Several protein kinase inhibitors (PKIs) are discovered with amine-substituted pyrimidines as their bioactive core (Fig. 1).[6–8]

A diversity-oriented synthesis (DOS) strategy[9–11] was employed to design a library of novel compounds with potential anti-cancer activity. Since DOS approach in medicinal chemistry aims to create structurally diverse molecules, it enhances the probability of discovering compounds with unique biological activities. Unlike traditional methods, DOS does not restrict itself to specific protein targets, thereby opening up new avenues for uncovering previously unidentified critical pathways involved in tumorigenesis. Recently, we have utilized this technique for the design of a novel quinazoline series where compounds had exhibited interesting properties with excellent anticancer activity against breast cancer cell lines while inflicting minimum effect on non-cancer cells.[12] In our current study, the 4-aminopyrazolo[3,4-*d*]pyrimidine scaffold was integrated with several structurally diverse biologically active fragments, starting from simple aromatics, halogen-substituted aromatics, heterocycles, polycyclic fragments, *etc.* The choice to combine multiple drug scaffolds into single molecules was driven by the hypothesis that this approach could (1) address drug resistance by bypassing common resistance pathways, (2) reduce the need for combination therapy, and (3) enhance efficacy by simultaneously targeting multiple pathways. Moreover, the compounds were subjected to high throughput *in vitro* screening against 60 human tumour cell lines consisting of the most extensive cancer pharmacology database.[13]

Due to our continuous efforts in identifying novel biologically active compounds,[14] we have synthesized novel derivatives

[a]*Sri Sathya Sai Institute of Higher Learning, Anantapur – 515 001, Andhra Pradesh, India*

[b]*SVAK Life Sciences, ALEAP Industrial Area, Pragathi Nagar, Hyderabad – 500090, India. E-mail: naveen071280@gmail.com*

[c]*Department of Chemistry, Faculty of Science, Umm Al-Qura University, Makkah 21955, Saudi Arabia*

† Electronic supplementary information (ESI) available. See DOI: https://doi.org/10.1039/d4ra05136j

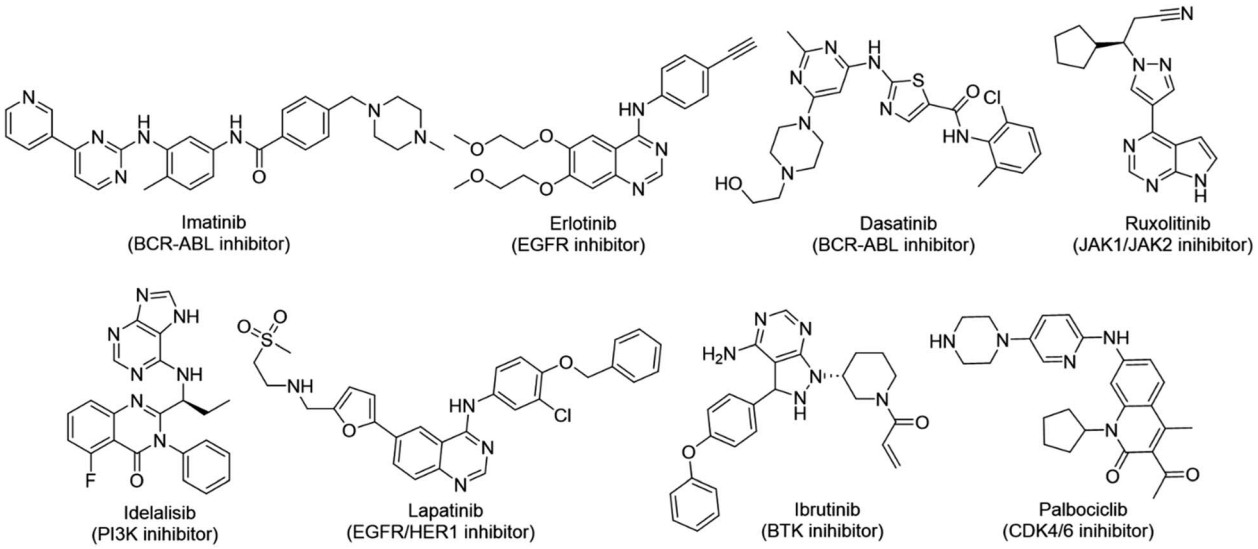

Fig. 1 Pyrimidines in small-molecule inhibitors used in selective killing of tumorigenic cells.

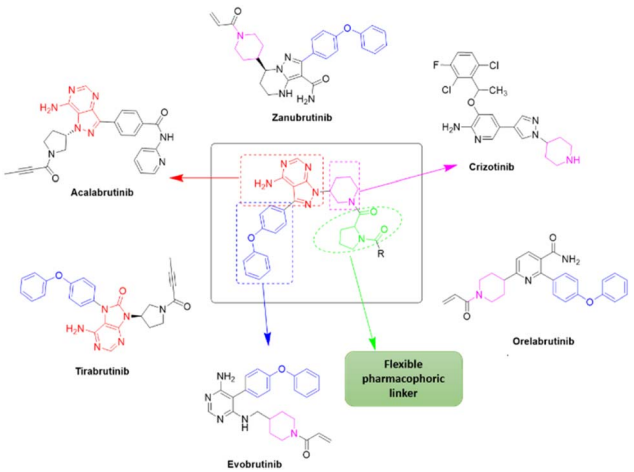

Fig. 2 Design model for the novel molecules.

containing 4-aminopyrazolo[3,4-*d*]pyrimidine (4-APP) scaffold, which is a privileged scaffold found in many biologically active compounds.[15–19] All the synthesized compounds under the present study were rigorously characterized using spectroscopic techniques such as ^{1}H NMR, ^{13}C NMR, IR and HRMS. Given our interest in exploring small molecules for their bioactivities,[20–23] we have considered the molecular skeleton of several small molecule inhibitors (SMIs) to design a new series of small molecules with a 4-APP core (Fig. 2). An evaluation of their growth inhibitory activities was performed against 60 human tumor cell lines belonging to nine different panels including leukaemia, non-small cell lung cancer (NSCLC), colon, central nervous system (CNS), melanoma, ovarian, renal, prostate, and breast cancer cell lines. Additionally, the structure–activity relationships were studied and the activities of the most active compounds were compared with that of the market drugs to understand how well the new compounds perform in relation to existing small molecule drugs.

Results and discussion

Chemistry

We followed the literature procedure to synthesize up to compound **8**.[24] Compound **8** was then reacted with Boc-proline to get compound **10**, which was deprotected using 1 M HCl to get the target core **11** (Scheme 1). Compound **11** was used as a starting material for synthesizing new derivatives. The synthetic sequences leading to the formation of novel pyrazolopyrimidine derivatives are illustrated in Scheme 2. The synthetic procedure of compound **8** was started from 4,6-dichloropyrimidine-5-carboxylic acid **1**. Compound **1** was converted to its corresponding acid chloride, followed by Friedel–Crafts acylation on diphenyl ether, which yielded compound **4**. Compound **4** on reaction with ammonia and hydrazine hydrate to produce pyrazolopyrimidine ring **5**. The pyrazolopyrimidine **5** was reacted with BOC-protected piperidin-3-ol **6** to give compound **7**, which was deprotected with HCl gave compound **8**. Compound **8** upon coupling with BOC-protected proline followed by deprotection with 1 M HCl gave a novel intermediate **11**. Derivatives were prepared from compound **11** using different acids to get required compounds. To prepare these derivatives, amide coupling was employed using appropriate reagent to carry out reactions between compound **11** with various carboxylic acids including aliphatic, aromatic, heteroaryl, and also polycyclic carboxylic acids.

The choice of reagent[25–27] for the amide coupling in the final step was optimized using different reaction conditions summarized in Table 1. The optimization for the choice of amide coupling reagent was performed by taking benzoic acid (**g**) and compound **11** as starting material. Several reagents such as DCC/HOBT, EDC/HOBT, and triphenylphosphine in the presence of iodine were considered. But the reaction time was either too long or the yield was unsatisfactory or tedious work up was involved during the usage of the above reagents. To optimize the reaction further, we have tested 2-(1*H*-

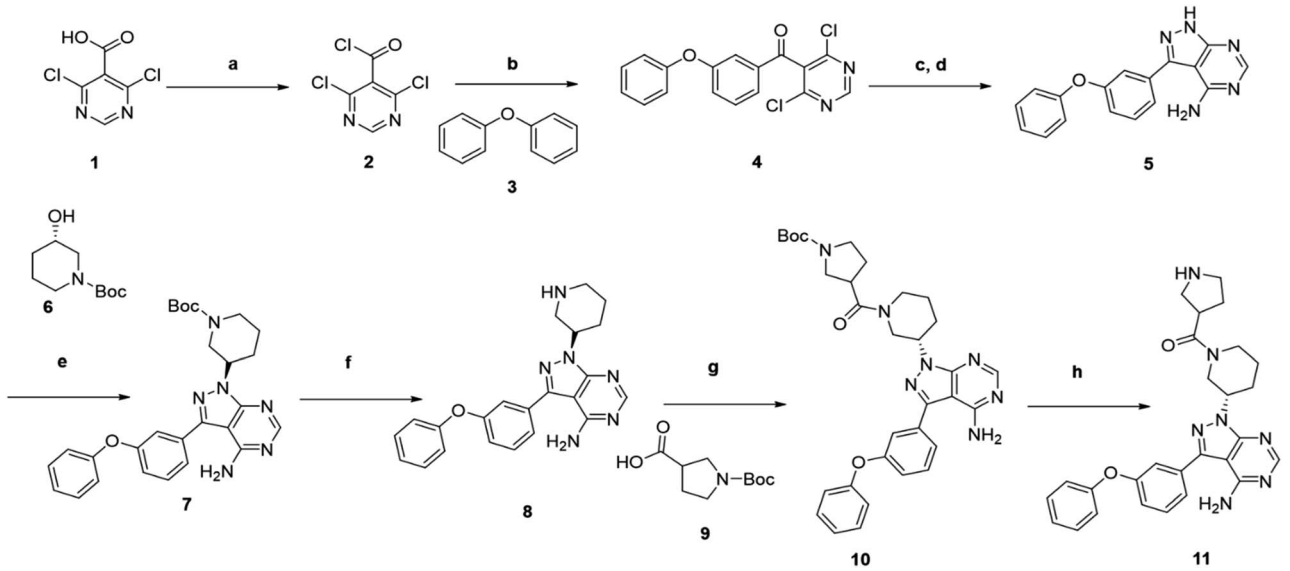

Scheme 1 Synthesis of novel 4-aminopyrazolo[3,4-*d*]pyrimidine amine derivative (**11**) that was used as starting material for the synthesis of the novel library.

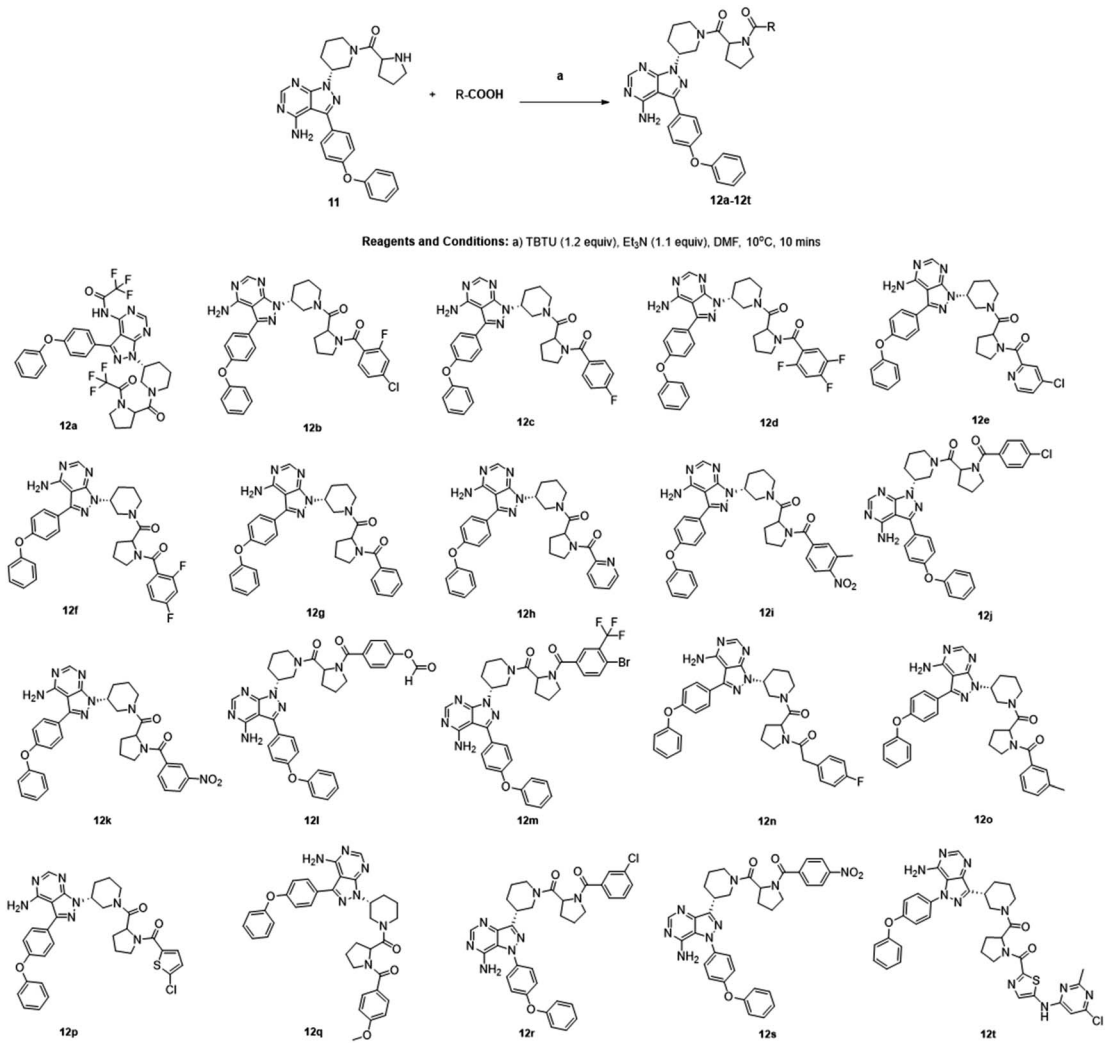

Scheme 2 Synthesis of novel pyrazolopyrimidine derivatives (**12a–12t**).

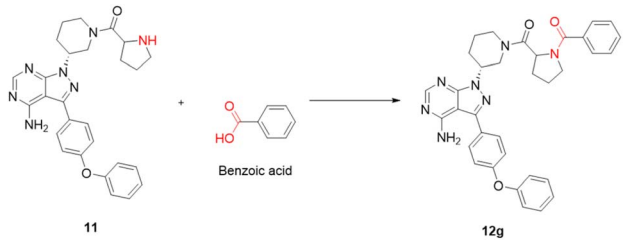

Scheme 3 Model reaction for the synthesis of **12g**.

benzotriazole-1-yl)-1,1,3,3-tetramethylammonium tetrafluoroborate[28] (TBTU) and *N*,*N*,*N*′,*N*′-tetramethyl-*O*-(1*H*-benzotriazol-1-yl)uronium hexafluorophosphate (HBTU) for coupling between benzoic acid (g) and compound **11**. TBTU, in the presence of triethylamine, was yielded 96% of the required product when compared with TBTU. So HBTU was found to be the best coupling reagent, which is yielding more than 80% of the required product in each reaction, and was chosen for the amide coupling reaction. The reaction was deemed successful with a wide variety of structurally diverse biologically active fragments, which proved the versatility of the reactions that are possible with the novel intermediate synthesized; depending on the structure of the carboxylic acids, the reaction time varied from five minutes to three hours (Scheme 3).

All the new molecules synthesized under this work were characterized using spectroscopic techniques, such as electron spray ionisation mass spectroscopy (HRMS), ^{1}H NMR, and ^{13}C NMR. The details are available in the ESI.†

Biological evaluation

The cells in the NCI-60 panel were extensively profiled at the DNA, RNA, protein, chromosomal, and functional level,[29–31] providing a diverse genotypic and karyotypic range of cell lines for screening new compounds. The single-dose data of the compounds were represented as a mean growth inhibition percentage (%GI) in Table 2. This preliminary screening allowed for the selection of compounds with exceptional anticancer properties for further investigation. Subsequently, compounds exhibiting outstanding anti-proliferative activity against many cell lines were chosen for the next phase. In this phase, the selected compounds were subjected to a dose-dependent study to determine the IC_{50} values across various cancer cell lines at different concentrations (100 μM, 10 μM, 1 μM, 0.1 μM, and 0.01 μM).

The single-dose study provided an overview of the anticancer activity of all the molecules under this study. Among the tested molecules, five compounds (**12c**, **12d**, **12f**, **12j**, and **12r**) were the most active and exhibited exceptional GI activity across all cell lines (Fig. 3). Compounds **12c**, **12d**, **12f**, **12i**, **12j**, **12m**, **12q**, and **12r** exhibited the best activity in the human melanoma cell line, *i.e.*, SK-MEL-5 (%GI > 100), whereas compounds **12d** and **12f** were the most active in HL-60 (TB) (GI% > 101) in the leukemia panel. Compound **11** showed selective growth inhibition in cell lines such as K-562 (%GI = 93) from leukemia, MALME-3M (%GI = 174) from melanoma, and MDA-MB-468 (%GI = 109) from the breast cancer panel. The compounds **12b** and **12r** displayed significant activity in cell lines including HL-60(TB) (%GI = 98 for **12b**), MOLT-4 (%GI = 94 for **12r**), and K-562 (%GI = 92 for **8**) in the leukaemia panel, HOP-92 (%GI = 82 for **12b**) in NSCLC panel, COLO205 (%GI = 105 for **12r**) in the colon cancer panel, SK-MEL-5 (%GI = 186 for **12r**) and UACC-257 (%GI = 108 for compound **8**) in melanoma panel, and BT-549 (%GI = 122 for **12r**) from breast cancer panel. Other compounds that exhibited selective activity were **12q** and **12s** (%GI = 155 and 96, respectively, in SK-MEL-5) in melanoma, **12g** (%GI = 91 in HL-60(TB)) in leukemia, **12i** (%GI = 93 in T-47D) in breast cancer panel. The compounds with %GI values which were beyond 100 correspond to lethality in the mentioned cell lines were considered as more active compounds against the corresponding cell lines. The average growth inhibition percentage was calculated for each of the compounds and the screening results from the single-dose study were summarized in Table 2.

From the five-dose study, the mean IC_{50} values (Table 3) revealed that **12j** was the most active compound, followed by **12c** as they exhibited growth inhibitory activity against most of the cell lines in the NCI60 panel. The cell lines in the leukemia cancer panel were found to be sensitive to all five test drugs

Table 1 Optimization of reaction conditions for the synthesis of 1-(2-((*R*)-3-(4-amino-3-(4-phenoxyphenyl)-1*H*-pyrazolo[3,4-*d*]pyrimidin-1-yl) piperidine-1-carbonyl)pyrrolidin-1-yl)-2-(4-fluorophenyl)ethan-1-one (**12g**)

Entry	Base	Reagent	Solvent[a]	Temperature (°C)	Reaction time	Yield[b] (%)
1	—	$SOCl_2$	DCM	0 to RT	18 h	48
2	Et_3N	$SOCl_2$	DCM	0 to RT	1 h	67
3	Et_3N	PPh_3, I_2	DCM	0 to RT	90 min	81
4	—	EDC/HOBT	DMF	70	18 h	66
5	Et_3N	EDC/HOBT	DMF	70	10 h	89
6	—	DCC/HOBT	ACN	20	12 h	69
7	Et_3N	DCC/HOBT	ACN	50	12 h	83
8	Et_3N	HBTU	DMF	10	10 min	96
9	NNM	TBTU	DMF	10	5 min	85
10	Et_3N	TBTU	DMF	10	5 min	95

[a] Choice of solvent is based on solubility and/or literature survey. [b] Yield was calculated after compound isolation and purification.

Table 2 Single-dose NCI-60 screening results exhibiting the %GI in the various tumour cell lines in response to treatment with compounds (**12a–12t**) at 10 μM concentration[a]

	Growth Inhibition percentage at 10 μM concentration of molecules																	
CELL PANELS / Compounds	**11**	**8**	**12b**	**12c**	**12d**	**12f**	**12g**	**12h**	**12i**	**12j**	**12k**	**12l**	**12m**	**12n**	**12p**	**12q**	**12r**	**12s**	**12t**
Leukemia																			
CCRF-CEM	71	66	64	89	80	85	77	67	72	90	77	31	51	36	47	63	66	72	10
HL-60(TB)	45	61	98	94	103	101	91	34	46	97	66	44	83	49	57	76	84	79	-8
K-562	93	92	83	88	87	91	65	74	59	89	74	63	73	62	65	77	87	80	21
MOLT-4	90	85	89	91	90	96	58	82	81	93	86	56	90	74	81	81	84	94	40
RPMI-8226	73	72	89	108	101	108	82	65	82	106	85	28	73	60	68	71	91	72	25
SR	-	-	66	76	78	87	21	75	60	67	66	-	-	-	-	-	-	-	-4
Non-Small Cell Lung Cancer																			
A549/ATCC	31	22	69	74	78	76	60	32	56	71	59	8	60	43	43	56	68	36	-1
EKVX	39	32	76	81	81	81	55	29	51	78	59	25	71	73	62	84	85	64	4
HOP-62	55	62	44	71	52	58	41	26	35	72	24	-10	35	16	13	35	63	30	1
HOP-92	97	103	82	94	93	97	68	48	49	87	61	-6	43	42	25	31	59	62	2
NCI-H226	63	66	65	95	72	83	74	59	56	91	63	20	75	50	81	76	89	75	10
NCI-H23	47	53	59	70	68	70	52	25	53	69	45	13	61	32	37	56	74	48	4
NCI-H322M	-	-	24	37	36	36	16	8	-3	56	20	-	-	-	-	-	-	-	1
NCI-H460	14	13	61	73	72	74	50	25	41	80	49	10	69	24	46	59	77	41	1
NCI-H522	53	44	45	73	63	67	56	45	52	78	46	24	46	26	27	44	61	33	0
Colon Cancer																			
COLO 205	77	89	83	102	104	107	67	70	71	110	63	28	97	29	48	77	105	46	-1
HCC-2998	31	70	53	71	69	58	41	13	29	74	39	-2	62	16	25	42	64	21	-13
HCT-116	62	70	78	84	75	73	71	59	78	92	68	39	85	53	68	77	85	68	1
HCT-15	47	41	80	87	89	85	74	52	66	89	70	34	81	62	52	77	85	55	2
HT29	82	86	71	80	78	77	66	54	58	85	62	30	81	38	51	62	88	50	3
KM12	86	88	80	92	82	89	79	74	58	91	74	28	56	23	39	60	75	54	6
SW-620	27	50	30	41	51	50	16	-1	10	53	17	-1	48	9	18	31	57	14	-10
CNS Cancer																			
SF-268	62	54	57	66	66	65	45	44	33	73	60	21	43	47	52	59	69	55	5
SF-295	45	53	81	108	89	87	66	38	65	123	63	19	81	75	66	97	121	51	9
SF-539	79	73	59	80	74	71	59	63	68	100	59	74	65	55	65	72	77	61	27
SNB-19	35	36	53	65	61	64	43	24	28	74	40	22	54	27	39	47	63	39	-1
SNB-75	51	51	45	51	61	52	26	22	11	51	44	43	55	36	40	51	59	40	1
U251	94	127	58	67	66	66	49	34	33	84	38	44	69	54	62	74	87	67	-1
Melanoma																			
LOX IMVI	-	-	79	98	90	90	81	67	65	134	76	-	-	-	-	-	-	-	15
MALME-3M	174	87	45	72	66	66	50	44	35	64	40	21	59	39	57	62	70	48	-15
M14	67	91	54	70	66	69	60	36	46	85	42	65	63	40	54	68	78	48	4
MDA-MB-435	-	-	63	79	76	74	65	48	45	95	60	-	-	-	-	-	-	-	0
SK-MEL-2	18	8	52	89	72	70	42	2	24	122	41	0	46	5	31	37	82	26	3
SK-MEL-28	143	52	50	62	61	67	55	32	43	87	47	18	57	30	48	59	74	44	-6
SK-MEL-5	38	51	90	141	102	118	86	78	81	167	76	32	148	76	97	152	186	96	9
UACC-257	164	109	52	76	58	65	39	24	29	108	39	11	48	19	79	43	76	34	-12
UACC-62	33	65	61	74	70	73	66	62	59	88	62	37	60	48	51	62	77	57	24
Ovarian Cancer																			
IGROV1	-	-	68	66	70	71	46	32	54	73	60	-	-	-	-	-	-	-	12
OVCAR-3	24	43	66	84	76	81	46	21	39	78	47	32	67	46	53	68	86	49	0
OVCAR-4	32	34	69	76	73	74	58	67	54	77	61	25	66	49	69	64	73	63	14
OVCAR-5	42	56	18	29	53	39	21	11	5	38	5	-13	48	13	1	17	51	12	-12
OVCAR-8	34	37	55	69	68	63	49	32	53	70	48	21	57	37	33	53	64	35	8
NCI/ADR-RES	14	26	64	72	76	72	57	32	55	74	53	13	74	43	50	62	80	51	5
SK-OV-3	47	57	58	77	69	67	26	9	32	74	36	-23	38	21	11	29	67	24	-12
Renal Cancer																			
786-0	68	65	57	68	67	65	61	51	44	77	57	45	54	35	31	51	53	39	8
A498	-13	8	29	39	44	47	13	4	0	41	7	8	40	2	37	30	61	21	-50
ACHN	47	72	65	79	86	77	55	37	43	79	53	14	76	34	52	54	85	50	7
CAKI-1	94	91	67	80	78	78	66	61	57	77	68	49	66	50	65	68	78	65	8
RXF 393	73	86	80	100	97	96	84	77	63	91	83	67	64	47	47	68	78	59	11
SN12C	68	73	82	95	87	92	85	73	74	90	78	41	75	53	61	73	83	67	11
TK-10	34	39	40	64	70	60	46	31	25	67	40	1	40	13	24	31	53	30	-25
UO-31	55	54	82	87	87	86	77	68	67	86	76	21	72	56	54	63	74	69	28
Prostate Cancer																			
PC-3	32	29	78	85	82	84	75	52	74	82	68	2	49	27	46	48	66	41	21
DU-145	65	63	50	73	61	62	48	10	26	76	53	55	85	63	75	79	87	68	3
Breast Cancer																			
MCF7	57	73	89	92	90	91	82	62	78	95	81	19	46	39	39	46	77	41	22
MDA-MB-231/ATCC	-	-	50	74	63	63	50	52	33	85	42	-	-	-	-	-	-	-	11
HS 578T	65	67	60	72	68	59	46	50	33	64	45	34	52	39	35	46	62	47	9
BT-549	71	61	52	83	62	56	76	60	72	95	66	43	76	53	70	98	122	103	15
T-47D	47	64	96	95	94	93	87	81	93	97	83	55	86	79	88	92	97	83	22
MDA-MB-468	109	105	61	104	74	81	64	42	54	89	62	41	89	64	66	69	87	78	4
Mean GI%	60	62	64	79	75	75	57	44	49	84	56	26	65	41	50	62	79	53	5

Colour Scale: -45 (Minimum) 50 (Median) 120 (Maximum)

[a] Values lower than zero (denoted by red) correspond to no effect on the specific cell line at 10 μM. Values greater than 100 (denoted by green) correspond to lethality on the specific cell line at 10 μM. '—' denotes that the compound(s) was not tested against the particular cell line(s).

under the study. Upon considering the individual activities of the molecules, the UO-31 cell line from the renal cancer panel was the most sensitive (**12c**, IC_{50} = 0.87 μM), followed by HL-60 (TB) (**12f**, IC_{50} = 1.41 μM) and MOLT-4 (IC_{50} = 1.51 μM) in the leukemia panel. Compound **12d** was most active against MOLT-4 (IC_{50} = 2.0 μM) and HL-60(TB) (IC_{50} = 2.63 μM) from leukemia panel. Compounds **12c** and **12j** were especially active in MOLT-4 (IC_{50} = 1.58 μM and 1.82, respectively). In the melanoma panel, compound **12j** was the most effective in inhibiting tumor growth. Certain cell lines exhibited selective sensitivity. For example, cell lines such as MOLT-4 in the leukemia panel and SK-MEL-5 in the melanoma panel were susceptible to all five drug agents in the study, but cell lines such as M14 in the melanoma cancer panel were affected by selective compounds (**11**, IC_{50} = 2.40 μM; **12f**, IC_{50} = 15.5 μM) only.

Fig. 4 highlights the compound's cytotoxicity trend. Comparing their cytotoxic activity, based on IC_{50} values, against established small-molecule drugs for renal cancer treatment reveals compelling results. Remarkably, compound **12c** demonstrated 2.88 times greater activity than sorafenib and

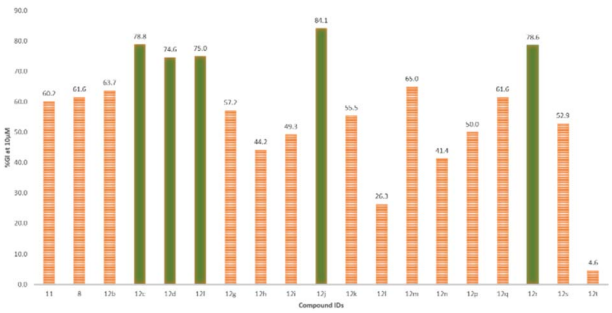

Fig. 3 Depiction of average %GI exhibited by all compounds in the study, highlighting the compounds with >75% growth inhibition (in green), at 10 μM concentration.

Table 3 Reduction in 50% of the net protein increase (IC_{50} in μM) as measured by SRB staining experiment by compounds across the tumour cell panels[a]

Cell Panel	Cell line	IC50 (μM) 12c	12d	12f	12j	11	IC50 (μM) Cladribine	Sunitinib	Sorafenib	Fludarabine	Cyclophosphamide
Leukemia	CCRF-CEM	3.47	4.90	7.59	3.31	7.08	0.06	6.46	2.29	2.34	208.93
	HL-60(TB)	1.70	2.63	1.41	2.09	6.31	0.07	2.40	1.51	3.63	181.97
	K-562	3.02	3.80	3.47	3.09	2.75	7.41	3.24	2.51	100.00	213.80
	MOLT-4	1.58	2.00	1.51	1.82	2.45	0.23	2.75	2.88	100.00	251.19
	RPMI-8226	2.24	4.07	2.69	2.51	5.01	23.99	4.57	1.55	100.00	251.19
Non-Small Cell Lung Cancer	A549/ATCC	5.37	5.01	9.33	4.17	10.96	2.04	2.95	2.95	38.90	251.19
	EKVX	5.37	5.89	6.17	4.79	12.30	4.07	5.25	2.69	100.00	251.19
	HOP-62	4.90	11.70	13.80	5.89	12.59	0.89	2.40	2.00	36.31	245.47
	HOP-92	4.90	4.37	4.79	3.89	5.62	0.79	-	1.74	32.36	245.47
	NCI-H226	3.72	5.50	5.01	4.17	6.17	12.02	5.75	2.00	100.00	251.19
	NCI-H23	6.46	8.91	9.77	7.24	10.96	0.47	2.57	1.95	10.23	234.42
	NCI-H322M	14.10	18.60	21.90	8.32	14.12	19.05	2.57	2.95	100.00	251.19
	NCI-H460	5.37	8.32	>100	6.46	14.12	5.50	2.19	2.45	52.48	251.19
	NCI-H522	17.40	20.00	21.90	15.80	8.13	7.41	3.55	2.04	53.70	251.19
Colon Cancer	COLO 205	5.25	6.03	4.90	3.89	4.68	7.39	2.95	2.34	54.95	251.19
	HCC-2998	6.17	10.50	12.30	4.37	11.48	5.75	2.95	2.82	3.98	190.55
	HCT-116	4.79	5.89	8.51	5.01	10.23	1.78	1.58	1.91	28.18	251.19
	HCT-15	5.01	4.79	6.76	3.72	11.48	9.12	1.23	2.63	75.86	251.19
	HT29	5.25	5.25	5.75	3.63	4.79	9.77	1.29	2.34	100.00	223.87
	KM12	5.25	61.70	20.40	5.25	3.39	43.65	0.10	1.78	91.20	251.19
	SW-620	12.00	27.50	12.30	14.50	11.75	6.17	1.95	2.88	66.07	251.19
CNS Cancer	SF-268	4.79	5.25	6.17	4.47	6.16	11.48	2.75	2.63	53.70	251.19
	SF-295	3.39	3.89	5.01	2.63	10.23	40.74	4.07	1.70	100.00	204.17
	SF-539	2.69	9.77	10.50	4.17	4.47	14.45	2.34	1.62	100.00	251.19
	SNB-19	11.00	11.20	17.00	5.62	13.18	1.55	5.37	3.47	100.00	251.19
	U251	7.94	7.24	13.20	4.90	8.91	6.61	3.09	2.14	75.86	251.19
Melanoma	LOX IMVI	3.47	5.01	4.79	3.09	2.57	3.09	2.29	1.66	9.33	251.19
	MALME-3M	3.98	15.10	6.92	7.08	4.57	100.00	2.19	2.14	51.29	251.19
	M14	11.50	12.90	15.50	5.13	2.40	0.19	1.02	2.19	6.31	251.19
	MDA-MB-435	6.17	7.24	10.20	3.55	7.76	0.54	1.62	1.82	11.22	251.19
	SK-MEL-2	11.00	11.50	11.50	5.75	14.80	100.00	2.09	1.78	100.00	251.19
	SK-MEL-28	4.07	>100	11.00	4.47	3.89	57.54	3.02	2.63	100.00	251.19
	SK-MEL-5	3.09	4.07	3.98	2.40	2.75	4.37	2.88	1.58	22.91	239.88
	UACC-257	>100	13.20	12.30	3.39	1.90	1.62	2.51	2.19	100.00	208.93
	UACC-62	3.63	4.57	4.27	3.39	6.46	0.55	3.24	1.70	97.72	251.19
Ovarian Cancer	IGROV1	5.25	11.50	6.92	5.62	6.76	45.71	2.63	2.63	89.13	251.19
	OVCAR-3	4.37	5.75	8.13	3.98	11.48	37.15	3.39	2.95	100.00	245.47
	OVCAR-5	10.20	17.00	17.00	12.30	6.17	1.91	2.34	3.09	100.00	251.19
	OVCAR-8	9.55	8.32	14.50	5.62	13.18	0.07	2.82	3.02	3.80	251.19
	NCI/ADR-RES	5.37	5.13	8.71	4.57	13.80	0.11	4.47	2.63	4.37	251.19
	SK-OV-3	6.31	10.70	13.80	5.13	6.03	19.95	2.29	2.51	30.20	251.19
Renal Cancer	786-0	18.20	12.30	22.90	7.24	6.61	2.45	3.09	3.47	-	251.19
	A498	7.41	6.03	13.20	9.12	16.22	4.07	2.19	2.14	100.00	239.88
	ACHN	2.95	6.76	7.08	4.57	8.32	0.56	1.55	2.63	27.54	251.19
	CAKI-1	3.89	3.63	3.63	3.63	5.13	0.54	1.05	2.88	6.46	199.53
	RXF 393	4.79	5.25	5.50	4.57	2.82	15.49	1.45	3.39	95.50	251.19
	SN12C	3.02	3.89	2.57	3.80	4.07	0.45	1.23	2.14	8.51	251.19
	TK-10	12.60	8.13	21.40	4.17	10.71	50.12	2.00	4.47	3.55	251.19
	UO-31	0.87	1.95	1.48	2.40	3.09	0.49	1.26	2.57	6.17	251.19
Prostate Cancer	PC-3	3.16	3.55	3.80	3.47	12.02	100.00	3.80	2.14	69.18	251.19
	DU-145	9.33	18.60	18.20	8.51	14.12	1.82	2.82	3.09	23.44	251.19
Breast Cancer	MCF7	3.31	3.63	3.16	2.69	4.27	3.55	2.24	2.82	52.36	251.19
	MDA-MB-231/ATCC	8.91	9.33	11.70	7.08	>100	79.43	3.24	1.32	100.00	251.19
	HS 578T	7.94	7.59	9.77	14.10	4.47	100.00	3.55	2.57	100.00	251.19
	BT-549	7.24	9.55	11.00	5.01	8.91	0.35	3.31	3.16	-	251.19
	T-47D	3.16	3.72	3.72	2.88	9.33	5.75	19.95	1.86	100.00	89.13
	MDA-MB-468	4.37	5.13	5.01	3.89	5.75	56.23	3.24	2.09	74.13	251.19
	Mean IC50 (in μM)	6.11	9.03	9.39	5.23	7.85	18.19	3.05	2.40	59.14	240.73

Lowest IC_{50} Highest IC_{50}

[a] The IC50 values equal to ">100" mean that the concentration required to achieve 50% activity has exceeded the highest tested concentration range, *i.e.*, 100 μM. Hence, the values for such cases are reported as either equal to or greater than 100 μM.

1.45 times greater activity than sunitinib. Detailed data is presented in Table 4, while Fig. 5 showcases a striking dose–response curve for compound **12c** in the highly sensitive UO-31 tumor cell line.

In summary, these findings underscore the potential of the candidate molecules as promising hit compounds, meriting comprehensive investigation to unravel their pharmacokinetics and pharmacodynamics, alongside evaluating their efficacy in animal model studies.

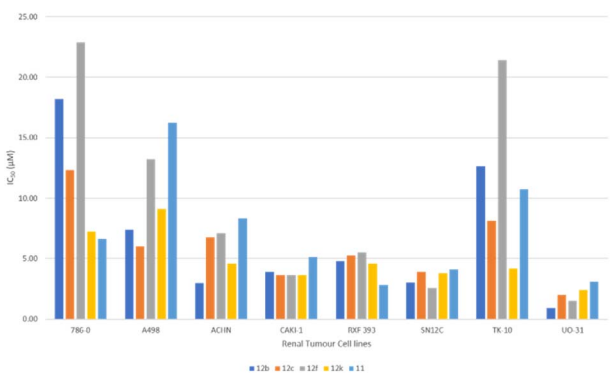

Fig. 4 Cytotoxic activity trend in renal cancer sub-panel depicting the IC_{50} value for compounds in the dose-dependent study.

Structure–activity relationships

The structure–activity correlation of the compounds was possible by comparing the %GI activity data obtained from the single-dose study. The study provided insights into the cytotoxic properties of the compounds in the presence of different substitutions in the pyrazolopyrimidine core. A graphical representation of the structure–activity correlation is depicted in Fig. 6. The introduction of simple heterocyclic acids on compound **8**, such as picolinic acid (**12h**) and 5-chlorothiophene-2-carboxylic acid (**12p**), showed only moderate activity. The presence of bulky heterocyclic groups such as 5-((6-chloro-2-methylpyrimidin-4-yl)amino)thiazole-2-carboxylic acid (**12t**) did not improve any activity. This data confirms that the presence of the heterocyclic moiety did not demonstrate any significant activity against cancer cell lines. On the other hand, introducing a simple benzoic acid (**12g**) provided an average growth inhibition of 57.2%. An activity comparison between **12l** (GI = 5%) and **12m** (GI = 65%) demonstrated that introducing halogen-substituted aromatic acids significantly improved the activity of the derivatives. Furthermore, introducing halogens at different positions of benzoic acid (as in **12d**) showed better activity than a trifluoro $-CF_3$ group (**12m**) substituted benzoic acid. The halogen substitution on benzoic acid showed good to better activity (as in **12c** and **12j**). Additionally, it was observed that replacing the fluorine with chlorine at the para position (as in compound **12j**) resulted in the best activity profile with an average growth inhibition of 84%. Other substitutions such as $-CH_3$, $-NO_2$, –OPh, $-OCH_3$ groups did not show any better activity. Fig. 7 summarizes the structure–activity correlation study.

Materials and methods

General procedures

The solvents and chemicals used in the spectroscopic studies were purchased from Sigma-Aldrich, Merck (Darmstadt, Germany). The melting points were determined in open capillary tubes using Labtronics Automatic Digital Melting Point Apparatus (Model: LT-109, Guelph, Canada). The molecular weights of the compounds were determined by understanding the mass spectra obtained using a mass spectrometer (Agilent 6550 tunnel QTOF Mass Spectrometer, California, USA). The purity of the compounds was confirmed by using Waters Binary HPLC System with a 1525 Binary HPLC Pump (Massachusetts, USA). ^{1}H NMR and ^{13}C NMR spectra were determined at 400 MHz and 100 MHz, respectively, using an NMR spectrometer (Bruker Ascend Avance III HD, Karlsruhe, Germany). Chemical shifts are expressed in δ (ppm).

Chemistry

A five-step synthesis was used for the preparation of compound **8**. The details for the same are reported elsewhere.[32] The progress of the reaction and the formation of products was monitored using thin layer chromatography till the formation of compound 7777.

Table 4 Anti-cancer activity comparison of the drug agents in terms of IC_{50} with market drugs that are currently in use for the treatment of renal cancer

	Renal cancer sub-panel (IC50 in μM)							
Compound ID (NSC ID)	786-0	A498	ACHN	CAKI-1	RXF 393	SN12C	TK-10	UO-31
12b (844710)	18.2	7.41	2.95	3.89	4.79	3.02	12.6	**0.87**
12c (844703)	12.3	6.03	6.76	3.63	5.25	3.89	8.13	1.95
12f (844704)	22.9	13.2	7.08	3.63	5.50	2.57	21.4	1.48
12j (844708)	7.24	9.12	4.57	3.63	4.57	3.8	4.17	2.40
11 (845676)	6.61	16.22	8.32	5.13	2.82	4.07	10.7	3.09
Sunitinib[a] (750690)	3.09	2.18	1.55	1.05	1.41	1.23	1.99	**1.26**
Sorafenib[a] (747971)	3.47	2.13	2.63	2.88	3.39	2.51	4.47	**2.57**

[a] The IC_{50} values for the standard drugs were obtained from the COMPARE database of DTP-NCI using their NSC IDs.

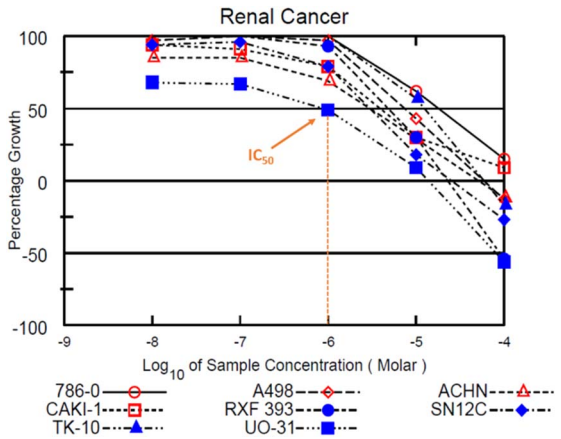

Fig. 5 Dose–response curves in the renal cancer sub-panel depicting the IC_{50} value for compound **12b** in UO-31 tumour cell line.

(*S*)-3-(3-Phenoxyphenyl)-1-(piperidin-3-yl)-1*H*-pyrazolo[3,4-*d*] pyrimidin-4-amine (8).

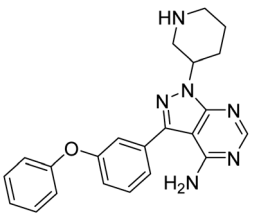

Compound 7 (61.65 mmol, 30 g) was dissolved in ethyl acetate and added with HCl (35–36%) at 50 °C, and stirred for 90 minutes. The solvent was evaporated under vacuum, residue, filtered and washed with ethyl acetate. The organic part was separated and evaporated under pressure to obtain compound **8.**

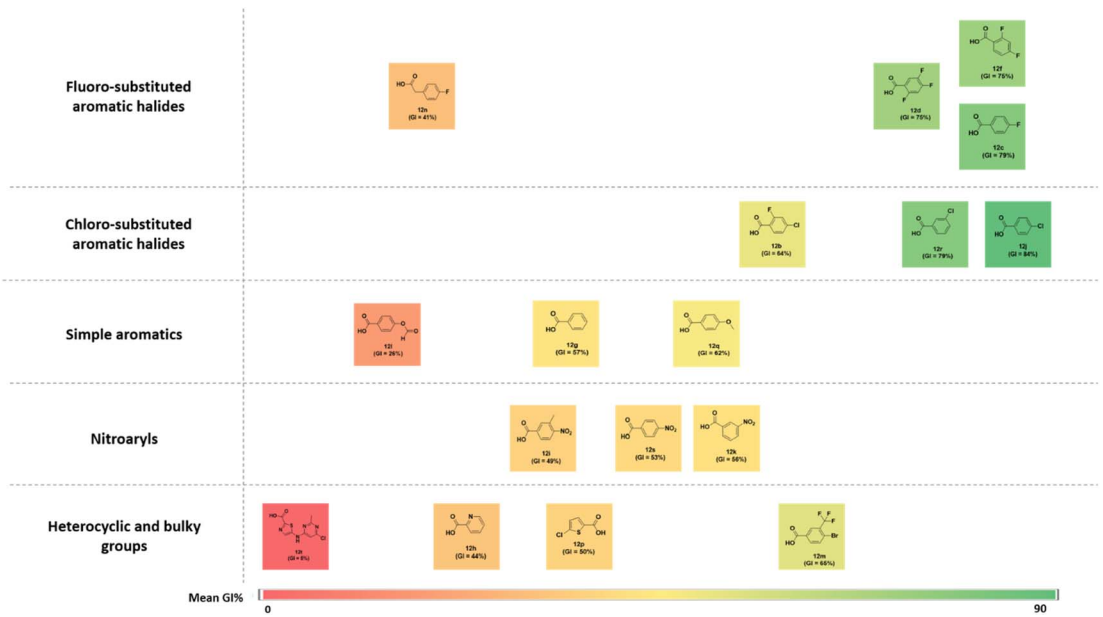

Fig. 6 Structure–activity correlation chart for synthesized compounds (**12a–12t**) based on NCI-60 average growth inhibition percentage (%GI).

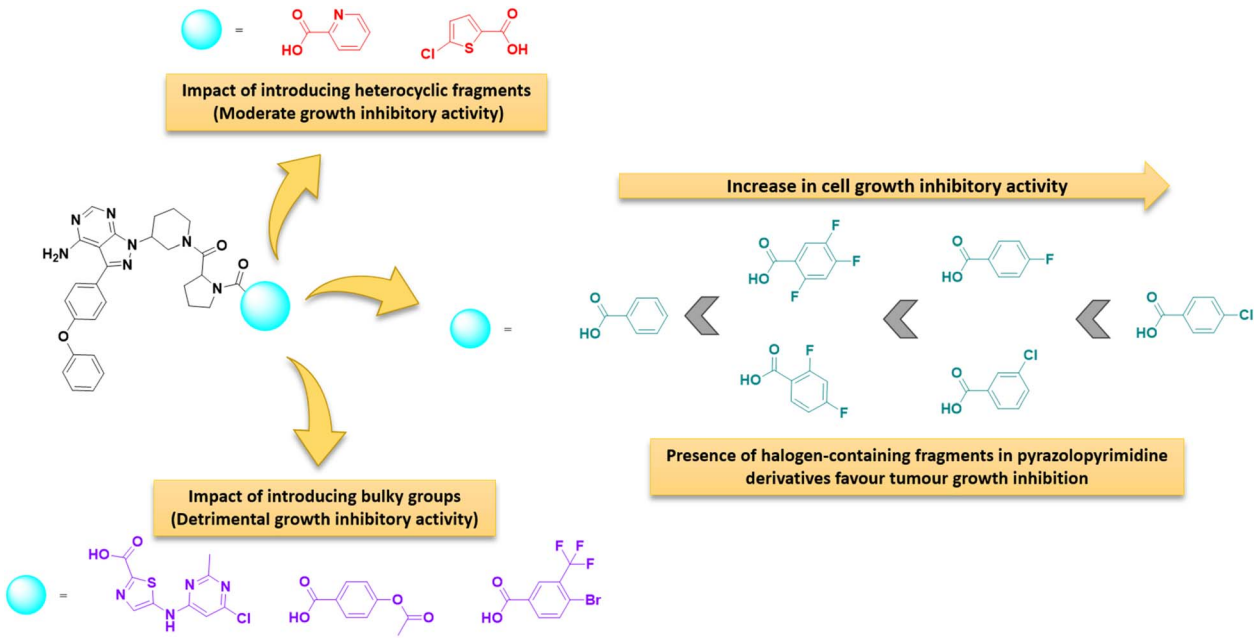

Fig. 7 Overview of structure–activity relationship.

Off-white powder; yield: 22.41 g (94%); m.p.: 142 °C; ^{1}H NMR (DMSO-D$_6$, 400 MHz): δ ppm 8.24 (1H, s, Ar–H), 7.65–7.67 (2H, d, J = 8 Hz), 7.42–7.46 (2H, t, J = 8 Hz, Ar–H), 7.12–7.21 (5H, m, Ar), 4.64–4.72 (1H, m, NH), 3.05–3.10 (1H, m, CH), 2.89–2.97 (2H, m, CH$_2$), 2.45–2.48 (2H, m, CH$_2$), 2.01–2.17 (2H, m, CH$_2$), 1.52–1.77 (2H, m, CH$_2$); ^{13}C NMR (DMSO-D$_6$, 100 MHz): δ ppm 158.6, 157.5, 156.8, 155.9, 154.2, 143.2, 130.6, 128.6, 124.2, 119.4, 97.8 54.4, 51.4, 45.9, 30.8 & 26.5; IR (KBr disc, cm^{-1}): 3475 s, 3295 s (N–H), 2952 s (sp^2 stretch), 2818 s (sp^3 stretch), 1646 s (C=O stretch), 1589 s (N–H bend), 1519 m, 1489 s, 1489 s (C–H bend), 1232 s (C–N stretch), 1167 w (C–O stretch), 870 w (N–H oop).

***tert*-Butyl 3-((*S*)-3-(4-amino-3-(3-phenoxyphenyl)-1*H*-pyrazolo[3,4-*d*]pyrimidin-1-yl)piperidine-1-carbonyl)pyrrolidine-1-carboxylate (10).**

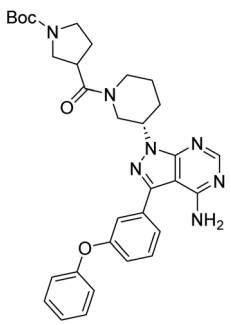

A solution of compound **8** (51.75 mmol, 20.45 g) in DMF was treated with Boc-proline **9** (51.75 mmol, 8 g) in the presence of triethylamine (14.5 mmol, 5.88 g) and TBTU (14.5 mmol, 18.8 g). The reaction mixture was stirred at 10–15 °C for 10 minutes. It was washed with water and ethyl acetate. The organic layer was separated and dried under a vacuum to obtain the title amine.

White powder; yield: 24.97 g (78%); m.p.: 145 °C; ^{1}H NMR (DMSO-D$_6$, 400 MHz): δ ppm 8.24–8.28 (1H, m, Ar), 7.65–7.67 (2H, d, J = 8 Hz, Ar–H), 7.42–7.46 (2H, t, J = 8 Hz, Ar–H), 7.12–7.21 (5H, m, Ar–H), 4.64–4.70 (1H, m, CH), 4.56–4.63 (1H, m, CH), 4.19–4.41 (2H, m, CH$_2$), 3.29–3.32 (2H, m, CH$_2$), 3.21–3.27 (2H, m, CH$_2$), 2.12–2.26 (2H, m, CH$_2$), 1.96–1.99 (2H, brs, CH$_2$), 1.70–1.83 (4H, m, CH$_2$), 1.40 (9H, s, CH$_3$); ^{13}C NMR (DMSO-D$_6$, 100 MHz): δ ppm 170.8, 158.7, 157.5, 156.8, 156.2, 154.4, 153.7, 143.7, 130.6, 128.4, 124.2, 119.4, 97.8, 78.8, 57.2, 56.8, 53.5, 52.4, 46.8, 46.3, 45.2, 30.2, 29.3, 28.6, 25.1 & 23.2; IR (KBr disc, cm^{-1}): 3478 s, 3300 s (N–H), 2951 s (sp^2 stretch), 2864 s (sp^3 stretch), 1628 s (C=O stretch), 1568 s (N–H bend), 1520 m, 1490 s (C–H bend), 1237 s (C–N stretch), 1165 w (C–O stretch), 872 w (N–H oop); mass: 584.33 [M + H]$^+$.

((*S*)-3-(4-Amino-3-(3-phenoxyphenyl)-1*H*-pyrazolo[3,4-*d*]pyrimidin-1-yl)piperidin-1-yl)(pyrrolidin-3-yl)methanone (11).

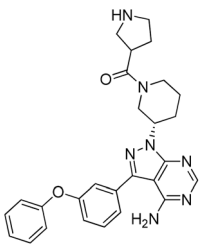

Compound **10** (16.57 mmol, 20 g) was dissolved in 1 M HCl in ethyl acetate (50 mL) and stirred at room temperature for 20 minutes. The reaction mixture was directly evaporated under a vacuum to obtain a white powder of the title amine that was then used for synthesizing the novel derivatives.

White powder; yield: 15 g (95%); m.p.: 148 °C; ^{1}H NMR (DMSO-D$_6$, 400 MHz): δ ppm 8.24–8.28 (1H, m, Ar–H), 7.65–7.68 (2H, m, Ar–H), 7.42–7.46 (2H, t, J = 8 Hz, Ar–H), 7.12–7.21 (5H,

m, Ar), 4.68–4.75 (1H, m, NH), 4.31–4.41 (1H, m, CH), 4.09–4.12 (1H, m, CH), 3.89–3.93 (2H, m, CH_2), 3.50–3.53 (2H, m, CH_2), 3.18–3.33 (2H, m, CH_2), 2.60–3.00 (2H, m, CH_2), 2.10–2.33 (2H, m, CH_2), 1.86–2.01 (2H, m, CH_2), 1.67 (2H, m, CH_2); ^{13}C NMR (DMSO-D_6, 100 MHz): δ ppm 172.2, 158.7, 157.5, 156.8, 156.1, 154.4, 143.7, 130.6, 128.4, 124.2, 119.5, 97.8, 66.8, 58.0, 52.3, 47.5, 46.2, 44.9, 42.0, 30.7, 29.9, 26.5 & 24.7; IR (KBr disc, cm^{-1}): 3471 s, 3304 s (N–H), 2939 s (sp^2 stretch), 2864 s (sp^3 stretch), 1639 s (C=O stretch), 1586 s (N–H bend), 1521 s, 1487 s (C–H bend), 1230 s (C–N stretch), 1167 w (C–O stretch), 869 w (N–H oop); Mass: calcd for $[C_{27}H_{29}N_7O_2]^+$ 483.56, found 482.26 [M–H].

General procedure for the synthesis of 12a–12t. The amine group in compound **11** was treated with various carboxylic acids to obtain derivatives **12a–12t**. To a solution of compound **11** (0.62 mmol, 300 mg) in *N*,*N*-dimethyl formamide (3 mL) at 10–15 °C, TBTU (0.68 mmol, 220 mg) and triethylamine (0.68 mmol, 69 mg) were added. The reaction mixture was stirred for about 10 minutes, the amine was added, and stirring was continued for five minutes to one hour. The progress of the reaction was monitored by TLC. The reaction mixture was washed with dilute $NaHCO_3$ solution. The precipitate so formed was filtered under vacuum, diluted with DCM, washed with hexane and distilled to get the title compounds.

*2,2,2-Trifluoro-N-(3-(4-phenoxyphenyl)-1-((3R)-1-(1-(2,2,2-trifluoroacetyl)pyrrolidine-2-carbonyl)piperidin-3-yl)-1H-pyrazolo[3,4-d]pyrimidin-4-yl)acetamide (**12a**).*

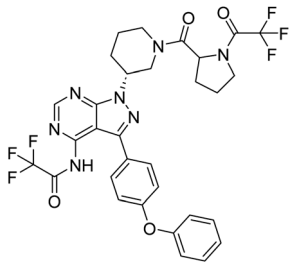

White powder; yield: 383.1 mg (91%); M.P.: 138 °C; ^{1}H NMR (DMSO-D_6, 400 MHz): δ ppm 8.23–8.31 (1H, m, Ar–H), 7.65–7.67 (1H, d, J = 8 Hz, Ar–H), 7.48–7.52 (1H, m, Ar–H), 7.42–7.46 (2H, t, J = 8 Hz, Ar–H), 7.11–7.21 (5H, m, Ar–H), 4.62–4.68 (1H, m, CH), 4.22–4.40 (1H, m, CH), 3.64–3.71 (2H, m, CH_2), 3.47–3.57 (2H, m, CH_2), 3.28–3.32 (2H, m, CH_2), 2.09–2.24 (2H, m, CH_2), 1.88–1.81 (2H, m, CH_2), 1.69–1.75 (2H, m, CH_2), 1.52–1.59 (2H, brs, CH_2); ^{13}C NMR (DMSO-D_6, 100 MHz): δ ppm 172.5, 170.3, 166.9, 158.6, 157.5, 156.8, 156.1, 143.6, 130.6, 128.4, 124.2, 119.4, 97.7, 56.8, 52.2, 33.9, 31.4, 28.9, 25.2, 22.5, 21.5 & 14.4; IR (KBr disc, cm^{-1}): 3486 s (N–H), 2929 s (sp^2 stretch), 2859 s (sp^3 stretch), 1634 s (C=O stretch), 1586 s (N–H bend), 1520 m, 1490 s, 1490 m, 1440 m (C–H bend), 1233 s (C–N stretch), 1151 w (C–O stretch), 849 w (N–H oop); HRMS: calcd for $[C_{31}H_{27}F_6N_7O_4]^+$ 675.5924, found 678.2410 [M − H + 2]$^+$, considering the isotopic fluorine substitution.

*4-Amino-1-((3R)-1-((4-chloro-2-fluorobenzoyl)prolyl)piperidin-3-yl)-3-(4-phenoxyphenyl)-1H-pyrazolo[3,4-d]pyrimidine (**12b**).*

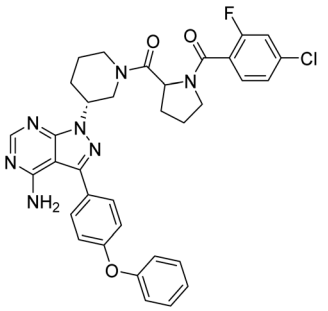

Cream colour powder; yield: 361.15 mg (91%); M.P.: 145 °C; ^{1}H NMR (DMSO-D_6): δ = ^{1}H NMR (DMSO-D_6, 400 MHz): δ ppm 8.25–8.36 (1H, m, Ar–H), 7.64–7.67 (2H, t, J = 8 Hz, Ar–H), 7.55–7.59 (1H, m, Ar–H), 7.39–7.45 (4H, m, Ar–H), 7.11–7.20 (5H, m, Ar), 4.92–5.04 (1H, m, CH), 4.61–4.73 (1H, m, CH), 4.19–4.33 (2H, m, CH), 3.58 (2H, brs, CH_2), 3.30–3.32 (2H, brs, CH_2), 2.26–2.32 (2H, brs, CH_2), 2.00–2.20 (2H, m, CH_2), 1.99–2.20 (2H, m, CH_2), 1.72–1.91 (4H, m, CH_2); ^{13}C NMR (DMSO-D_6, 100 MHz): δ ppm 158.6, 156.8, 143.8, 130.6, 128.4, 125.7, 124.2, 119.4, 56.9, 52.2, 32.0, 30.6, 29.5, 29.2, 24.7, 22.6 & 14.4; IR (KBr disc, cm^{-1}): 3475 s, 3317 s (N–H), 3206 s (sp^2 stretch), 2925 s (sp^3 stretch), 1632 s (C=O stretch), 1588 s (N–H bend), 1521 m, 1478 m, 1438 m (C–H bend), 1222 s (C–N stretch), 1166 w (C–O stretch), 860 w (N–H oop), 801 w (C–Cl stretch); HRMS: calcd for $[C_{34}H_{31}ClFN_7O_3]^+$ 640.1164, found 640.2217 [M + 1]$^+$ and 662.2043 [M + 1 + Na]$^+$.

*4-Amino-1-((3R)-1-((4-fluorobenzoyl)prolyl)piperidin-3-yl)-3-(4-phenoxyphenyl)-1H-pyrazolo[3,4-d]pyrimidine (**12c**).*

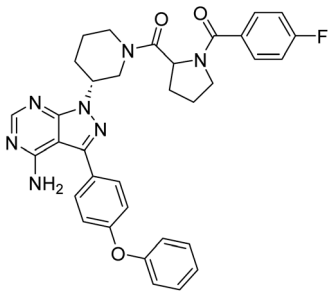

White powder; yield: 337.96 mg (90%); M.P.: 147 °C; ^{1}H NMR (DMSO-D_6, 400 MHz): δ ppm 8.24–8.33 (1H, m, Ar–H), 7.55–7.70 (4H, m, Ar–H), 7.42–7.45 (2H, t, J = 8 Hz, Ar–H), 7.36–7.39 (1H, m, Ar–H), 7.27–7.31 (1H, t, J = 8 Hz, Ar–H), 7.11–7.21 (5H, m, Ar–H), 4.91–5.04 (1H, m, CH), 4.72–4.79 (1H, m, CH), 4.25–4.46 (2H, m, CH_2), 3.48–3.62 (2H, m, CH_2), 3.30 (2H, brs, CH_2), 2.08–2.29 (2H, m, CH_2), 1.91–2.01 (4H, m, CH_2), 1.75–1.77 (2H, brs, CH_2); ^{13}C NMR (DMSO-D_6, 100 MHz): δ ppm 172.5, 170.2, 2.5, 170.2, 167.1, 158.7, 156.8, 156.1, 143.7, 133.5, 130.6, 130.2, 129.5, 128.4, 124.2, 119.5, 115.8, 97.7, 60.0, 57.2, 50.2, 45.6, 29.5, 29.0, 25.5 & 21.5; IR (KBr disc, cm^{-1}): 3476 s, 3304 s (N–H), 3186 s (sp^2 stretch), 2924 s (sp^3 stretch), 1621 s (C=O stretch), 1587 s (N–H bend), 1520 m, 1477 s, 1489 s (C–H bend), 1221 s (C–N stretch), 1141 w (C–O stretch), 862 w (N–H oop); HRMS: calcd for $[C_{34}H_{32}FN_7O_3]^+$ 605.6744, found 606.2617 [M + 1]$^+$ and 638.2439 [M + 1 + Na]$^+$.

*4-Amino-3-(4-phenoxyphenyl)-1-((3R)-1-((2,4,5-trifluorobenzoyl)prolyl)piperidin-3-yl)-1H-pyrazolo[3,4-d]pyrimidine (**12d**).*

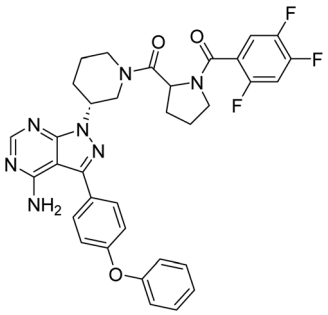

White powder; yield: 366.0 mg (92%); M.P.: 143 °C; ^{1}H NMR (DMSO-D$_6$, 400 MHz): δ ppm 8.25–8.31 (1H, m, Ar–H), 7.66–7.68 (2H, m, Ar–H), 7.44 (3H, brs, Ar–H), 7.28 (1H, brs, Ar–H), 7.14–7.17 (5H, m, Ar–H), 4.95–5.05 (1H, m, CH), 4.75 (1H, brs, CH), 4.15–4.45 (2H, m, CH$_2$), 3.51–3.69 (2H, m, CH$_2$), 2.95–3.15 (2H, m, CH$_2$), 2.26–2.33 (2H, m, CH$_2$), 1.90–2.18 (4H, brs, CH$_2$), 1.75–1.81 (2H, m, CH$_2$); ^{13}C NMR (DMSO-D$_6$, 100 MHz): δ ppm 170.0, 158.7, 157.5, 156.8, 156.2, 154.3, 143.8, 130.6, 128.3, 124.4, 119.4, 52.2, 49.0, 45.5, 30.6, 29.5, 24.7, 22.9, 17.7 & 14.2; IR (KBr disc, cm^{-1}): 3476 s, 3317 s (N–H), 3206 s (sp^2 stretch), 2925 s (sp^3 stretch), 1632 s (C=O stretch), 1588 s (N–H bend), 1519 m, 1478 s, 1438 s (C–H bend), 1222 s (C–N stretch), 1141 w (C–O stretch), 860 w (N–H oop); HRMS: calcd for $[C_{34}H_{30}F_3N_7O_3]^+$ 641.6552, found 642.2437 $[M + H]^+$.

*4-Amino-1-((3R)-1-((4-chloropicolinoyl)prolyl)piperidin-3-yl)-3-(4-phenoxyphenyl)-1H-pyrazolo[3,4-d]pyrimidine (**12e**).*

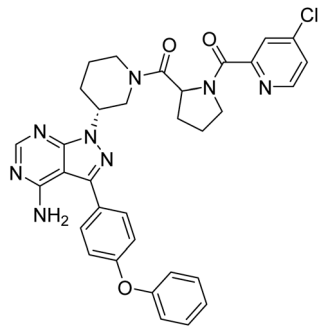

White powder; yield: 328.4 mg (85%); M.P.: 155 °C; ^{1}H NMR (DMSO-D$_6$, 400 MHz): δ ppm 8.60–8.65 (1H, m, Ar–H), 8.25–8.29 (1H, m, Ar–H), 7.82–7.84 (1H, m, Ar), 7.63–7.74 (3H, m, Ar–H), 7.42–7.46 (2H, t, J = 8 Hz, Ar–H), 7.11–7.19 (5H, m, Ar), 5.48–5.56 (1H, m, CH), 4.72–5.08 (1H, m, CH), 4.17–4.36 (2H, m, CH$_2$), 3.62–3.89 (2H, m, CH$_2$), 2.33–2.38 (2H, m, CH$_2$), 2.12–2.20 (2H, m, CH$_2$), 1.91 (2H, brs, CH$_2$), 1.79–1.87 (4H, m, CH$_2$); ^{13}C NMR (DMSO-D$_6$, 100 MHz): δ ppm 172.5, 170.3, 164.7, 158.7, 156.8, 156.1, 155.7, 154.3, 150.2, 149.6, 144.5, 143.7, 130.6, 128.4, 126.0, 124.3, 119.5, 97.8, 60.0, 52.2, 49.9, 48.8, 44.9, 31.4, 29.5, 21.5 & 14.4; IR (KBr disc, cm^{-1}): 3470 s, 3398 s (N–H), 2922 s (sp^2 stretch), 2856 s (sp^3 stretch), 1628 s (C=O stretch), 1570 s (N–H bend), 1489–1438 s (C–H bend), 1236 s (C–N stretch), 1166 w (C–O stretch), 845 w (N–H oop), 802 w (C–Cl); HRMS: calcd for $[C_{33}H_{31}ClN_8O_3]^+$ 623.1140, found 623.2252 $[M]^+$ and 625.2246 $[M + 2]^+$.

*4-Amino-1-((3R)-1-((2,4-difluorobenzoyl)prolyl)piperidin-3-yl)-3-(4-phenoxyphenyl)-1H-pyrazolo[3,4-d]pyrimidine (**12f**).*

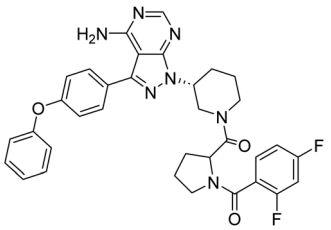

White powder; yield: 367.3 mg (95%); M.P.: 146 °C; ^{1}H NMR (DMSO-D$_6$, 400 MHz): δ ppm 8.25–8.35 (1H, m, Ar–H), 7.64–7.70 (2H, m, Ar–H), 7.41–7.45 (3H, t, J = 8 Hz, Ar–H), 7.33–7.38 (1H, m, Ar–H), 7.11–7.21 (6H, m, Ar–H), 4.91–5.05 (1H, m, CH), 4.63–4.74 (1H, m, CH), 4.21–4.46 (2H, m, CH$_2$), 3.57–3.62 (2H, m, CH$_2$), 3.29–3.32 (2H, m, CH$_2$), 2.14–2.32 (2H, m, CH$_2$), 1.91–2.03 (2H, m, CH$_2$), 1.73–1.85 (4H, m, CH$_2$); ^{13}C NMR (DMSO-D$_6$, 100 MHz): δ ppm 170.1, 169.9, 164.1, 163.1, 158.7, 157.7, 156.8, 154.4, 130.6, 128.4, 124.2, 119.5, 105.0, 97.7, 58.9, 56.9, 52.2, 47.1, 45.6, 30.0, 29.1, 24.7 & 22.9; IR (KBr disc, cm^{-1}): 3477 s, 3306 s (N–H), 2951 s (sp^2 stretch), 2855 s (sp^3 stretch), 1623 s (C=O stretch), 1567 s (N–H bend), 1521 m, 1487 s, 1427 s (C–H bend), 1239 s (C–N stretch), 1089 w (C–O stretch), 842 w (N–H oop); HRMS: calcd for $[C_{34}H_{31}F_2N_7O_3]^+$ 623.6648, found 624.2516 $[M + 1]^+$ and 625.2538 $[M + 2]^+$.

*4-Amino-1-((3R)-1-(benzoylprolyl)piperidin-3-yl)-3-(4-phenoxyphenyl)-1H-pyrazolo[3,4-d]pyrimidine (**12g**).*

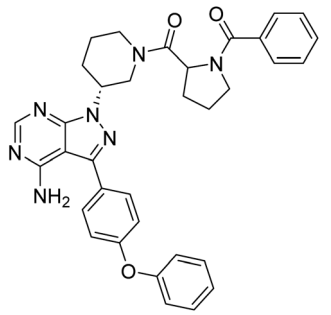

White powder; yield: 302.4 mg (83%); M.P.: 148 °C; ^{1}H NMR (DMSO-D$_6$, 400 MHz): δ ppm 8.24–8.34 (1H, m, Ar–H), 7.64–7.68 (2H, t, J = 8 Hz, Ar–H), 7.52–7.53 (2H, m, Ar–H), 7.44–7.47 (4H, t, J = 8 Hz, Ar–H), 7.35–7.36 (1H, d, J = 8 Hz, Ar–H), 7.14–7.16 (5H, m, Ar–H), 4.93–5.04 (1H, m, CH), 4.74 (1H, brs, CH), 4.02–4.47 (2H, m, CH$_2$), 3.47–3.60 (2H, m, CH$_2$), 2.95–3.12 (2H, m, CH$_2$), 2.26–2.30 (2H, m, CH$_2$), 1.88–2.16 (4H, m, CH$_2$), 1.76 (2H, brs, CH$_2$); ^{13}C NMR (DMSO-D$_6$, 100 MHz): δ ppm 169.8, 168.1, 158.7, 157.5, 156.8, 156.1, 154.3, 137.2, 130.6, 128.7, 127.5, 127.0, 124.2, 119.5, 97.8, 59.5, 57.0, 52.2, 50.2, 45.7, 30.0, 29.0, 25.4 & 24.7; IR (KBr disc, cm^{-1}): 3471 s, 3301 s (N–H), 2926 s (sp^2 stretch), 2959 s (sp^3 stretch), 1626 s (C=O stretch), 1568 s (N–H bend), 1523 m, 1476 s, 1434 s (C–H bend), 1221 s (C–N stretch), 1141 w (C–O stretch), 861 w (N–H oop); HRMS: calcd for $[C_{34}H_{33}N_7O_3]$ 587.6840, found 588.2705 $[M + H]^+$.

*4-Amino-3-(4-phenoxyphenyl)-1-((3R)-1-(picolinoylprolyl)piperidin-3-yl)-1H-pyrazolo[3,4-d]pyrimidine (**12h**).*

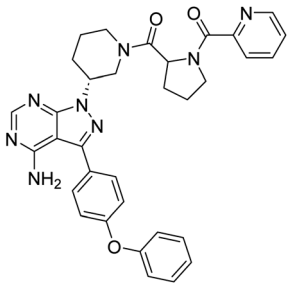

Yellowish-white powder; yield: 302.9 mg (83%); M.P.: 156 °C; ^{1}H NMR (DMSO-D$_6$, 400 MHz): δ ppm 8.60–8.65 (1H, m, Ar–H), 8.24–8.29 (1H, m, Ar–H), 7.93–8.01 (1H, m, Ar–H), 7.76–7.83 (1H, m, Ar–H), 7.64–7.69 (2H, m, Ar–H), 7.50–7.58 (1H, m, Ar–H), 7.42–7.46 (2H, t, J = 8 Hz, Ar–H), 7.12–7.21 (5H, m, Ar–H), 5.55–5.56 (1H, m, CH), 4.71–4.76 (1H, m, CH), 4.24–4.38 (2H, m, CH$_2$), 3.62–3.87 (2H, m, CH$_2$), 3.14–3.33 (2H, m, CH$_2$), 2.45–2.29 (2H, m, CH$_2$), 2.11–2.21 (2H, m, CH$_2$), 1.88–1.99 (2H, m, CH$_2$), 1.68–1.79 (2H, m, CH$_2$); ^{13}C NMR (DMSO-D$_6$, 100 MHz): δ ppm 170.5, 165.9, 158.7, 157.5, 156.8, 156.1, 154.2, 148.5, 147.9, 143.7, 137.8, 130.6, 128.4, 125.7, 124.6, 124.2, 119.4, 97.7, 59.6, 52.3, 49.9, 48.5, 44.9, 31.4, 30.0, 25.4 & 22.0; IR (KBr disc, cm^{-1}): 3466 s, 3397 s (N–H), 2925 s (sp^2 stretch), 2855 s (sp^3 stretch), 1623 s (C=O stretch), 1587 s (N–H bend), 1523 m, 1489 s, 1425 s (C–H bend), 1235 s (C–N stretch), 1133 w (C–O stretch), 801 w (N–H oop); HRMS: calcd for $[C_{33}H_{32}N_8O_3]^+$ 588.6720, found 589.2654 $[M + H]^+$.

*4-Amino-1-((3R)-1-((3-methyl-4-nitrobenzoyl)prolyl)piperidin-3-yl)-3-(4-phenoxyphenyl)-1H-pyrazolo[3,4-d]pyrimidine (**12i**).*

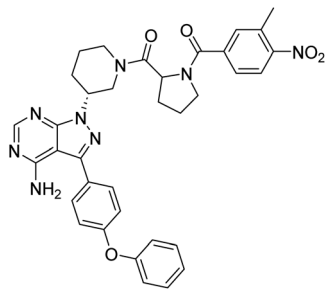

Yellowish-white powder; yield: 316.7 mg (80%); M.P.: 152 °C; ^{1}H NMR (DMSO-D$_6$, 400 MHz): δ ppm 8.24–8.30 (1H, m, Ar), 7.97–8.07 (1H, m, Ar), 7.77–7.83 (1H, m, Ar–H), 7.66–7.71 (2H, m, Ar–H), 7.60–7.65 (1H, m, Ar–H), 7.41–7.45 (2H, t, J = 8 Hz, Ar–H), 7.11–7.20 (5H, m, Ar–H), 4.96–5.05 (1H, m, CH), 4.72–4.75 (1H, m, CH), 3.92–4.46 (2H, m, CH$_2$), 3.51–3.64 (2H, m, CH$_2$), 2.64–2.57 (2H, m, CH$_2$), 2.16–2.33 (2H, m, CH$_2$), 1.99–2.03 (2H, m, CH$_2$), 1.78–1.91 (4H, m, CH$_2$), 1.23 (3H, s, CH$_3$); ^{13}C NMR (DMSO-D$_6$, 100 MHz): δ ppm 170.1, 165.8, 158.6, 157.5, 156.8, 156.0, 149.1, 143.7, 137.1, 136.0, 134.6, 133.5, 132.1, 130.6, 128.3, 124.4, 123.5, 119.5, 97.7, 60.0, 57.4, 52.1, 50.1, 47.6, 31.4, 22.5, 22.5, 20.0 & 14.4; IR (KBr disc, cm^{-1}): 3466 s (N–H), 2925 s (sp^2 stretch), 2855 s (sp^3 stretch), 1623 s (C=O stretch), 1587 s (N–H bend), 1523 m, 1489 s (C–H bend), 1235 s (C–N stretch), 1133 w (C–O stretch), 801 w (N–H oop); HRMS: calcd for $[C_{35}H_{34}N_8O_5]^+$ 646.7080, found 647.2712 $[M + H]^+$.

*4-Amino-1-((3R)-1-((4-chlorobenzoyl)prolyl)piperidin-3-yl)-3-(4-phenoxyphenyl)-1H-pyrazolo[3,4-d]pyrimidine (**12j**).*

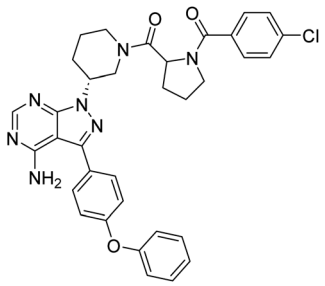

White powder; yield: 339.4 mg (88%); M.P.: 148 °C; ^{1}H NMR (DMSO-D$_6$, 400 MHz): δ ppm 8.23–8.34 (1H, m, Ar–H), 7.61–7.70 (3H, m, Ar–H), 7.51–7.57 (2H, m, Ar–H), 7.42–7.45 (2H, t, J = 8 Hz, Ar–H), 7.37–7.39 (1H, d, J = 8 Hz, Ar–H), 7.11–7.20 (5H, m, Ar–H), 5.01–5.04 (1H, m, CH), 4.72–4.77 (1H, m, CH), 4.24–4.35 (1H, m, CH), 3.46–3.62 (2H, m, CH$_2$), 2.26–2.33 (2H, m, CH$_2$), 2.10–2.16 (2H, m, CH$_2$), 1.75–1.91 (4H, m, CH$_2$), 1.47–1.60 (2H, m, CH$_2$); ^{13}C NMR (DMSO-D$_6$, 100 MHz): δ ppm 170.6, 158.7, 156.8, 156.1, 130.6, 129.6, 129.1, 129.0, 128.8, 128.4, 124.4, 119.5, 57.1, 52.2, 34.7, 31.4, 29.0, 26.8, 25.2, 22.5 & 14.4; IR (KBr disc, cm^{-1}): 3477 s, 3306 s (N–H), 2951 s (sp^2 stretch), 2866 s (sp^3 stretch), 1623 s (C=O stretch), 1566 s (N–H bend), 1521 m, 1427 s (C–H bend), 1239 s (C–N stretch), 1167 w (C–O stretch), 844 w (N–H oop), 803 w (C–Cl stretch); HRMS: calcd for $[C_{34}H_{32}ClN_7O_3]^+$ 622.1260, found 622.2297 $[M]^+$ and 644.2124 $[M + Na]^+$.

*4-Amino-1-((3R)-1-((3-nitrobenzoyl)prolyl)piperidin-3-yl)-3-(4-phenoxyphenyl)-1H-pyrazolo[3,4-d]pyrimidine (**12k**).*

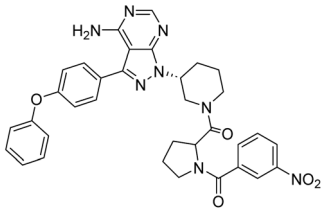

Yellowish-white powder; yield: 321.6 mg (82%); M.P.: 152 °C; ^{1}H NMR (DMSO-D$_6$, 400 MHz): δ ppm 8.34–8.39 (1H, m, Ar), 8.16–8.29 (1H, m, Ar), 7.89–8.03 (1H, m, Ar–H), 7.76–7.84 (1H, m, Ar–H), 7.61–7.70 (2H, m, Ar–H), 7.41–7.44 (2H, t, J = 8 Hz, Ar–H), 7.11–7.18 (5H, m, Ar–H), 4.97–5.07 (1H, m, CH), 4.63–4.76 (1H, m, CH), 3.89–4.47 (2H, m, CH$_2$), 3.60–3.63 (2H, m, CH$_2$), 3.40–3.49 (2H, m, CH$_2$), 2.16–2.34 (2H, m, CH$_2$), 1.93–2.06 (2H, m, CH$_2$), 1.78–1.86 (4H, m, CH$_2$); ^{13}C NMR (DMSO-D$_6$, 100 MHz): δ ppm 170.1, 166.0, 158.7, 157.5, 156.8, 156.2, 154.3, 148.0, 143.7, 139.6, 138.5, 133.9, 130.6, 128.3, 125.1, 124.2, 122.3, 119.5, 97.7, 59.6, 57.4, 52.0, 47.6, 46.5, 31.4, 25.4, 22.5 & 14.4; IR (KBr disc, cm^{-1}): 3476 s, 3306 s (N–H), 2946 s (sp^2 stretch), 2869 s (sp^3 stretch), 1624 s (C=O stretch), 1568 s (N–H bend), 1531 m, 1489 s (C–H bend), 1349 s (N–O stretch), 1236 s (C–N stretch), 1164 w (C–O stretch), 868 w (N–H oop); HRMS: calcd for $[C_{34}H_{32}N_8O_5]^+$ 632.6810, found 633.2564 $[M + 1]^+$.

*4-(2-((R)-3-(4-amino-3-(4-phenoxyphenyl)-1H-pyrazolo[3,4-d]pyrimidin-1-yl)piperidine-1-carbonyl)pyrrolidine-1-carbonyl) phenyl acetate (**12l**).*

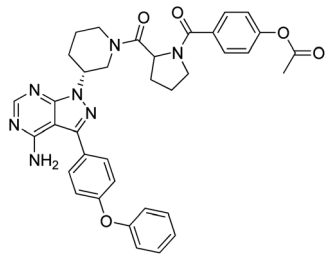

White powder; yield: 86%; M.P.: 344.3 mg (86%); ^{1}H NMR (DMSO-D_6, 400 MHz): δ ppm 8.22–8.30 (2H, m, Ar–H), 7.65–7.67 (3H, m, Ar–H), 7.39–7.46 (4H, m, Ar–H), 7.12–7.20 (5H, m, Ar–H), 4.95–5.06 (1H, m, CH), 4.70–4.83 (1H, m, CH), 4.27–4.36 (2H, m, CH_2), 3.89–4.06 (2H, m, CH_2), 3.48–3.60 (2H, m, CH_2), 3.18–3.24 (2H, m, CH_2), 2.24–2.33 (2H, m, CH_2), 2.10–2.13 (2H, m, CH_2), 1.91–1.96 (3H, m, CH_3), 1.78–1.83 (2H, m, CH_2), 1.56–1.68 (2H, m, CH_2); ^{13}C NMR (DMSO-D_6, 100 MHz): δ ppm 170.7, 158.7, 157.4, 156.8, 154.4, 132.2, 130.6, 128.4, 124.2, 123.1, 122.3, 119.5, 97.7, 56.2, 47.9, 46.5, 34.6, 31.4, 30.0, 25.2, 24.6 & 22.7; IR (KBr disc, cm^{-1}): 3471 s, 3301 s (N–H), 2926 s (sp^2 stretch), 2859 s (sp^3 stretch), 1626 s (C=O stretch), 1568 s (N–H bend), 1523 m, 1476 s, 1434 w (C–H bend), 1221 s (C–N stretch), 1141 w (C–O stretch), 861 w (N–H oop); HRMS: calcd for $[C_{36}H_{35}N_7O_5]^+$ 645.2760, found 646.2770 $[M + H]^+$.

*4-Amino-1-((3R)-1-((4-bromo-3-(trifluoromethyl)benzoyl)prolyl) piperidin-3-yl)-3-(4-phenoxyphenyl)-1H-pyrazolo[3,4-d]pyrimidine (**12m**).*

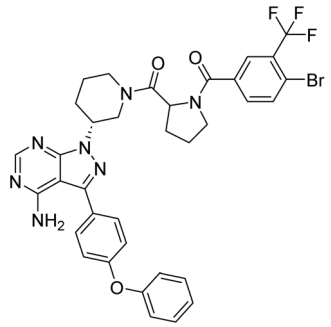

White powder; yield: 437.2 mg (96%); M.P.: 146 °C; ^{1}H NMR (DMSO-D_6, 400 MHz): δ ppm 8.23–8.33 (1H, m, Ar–H), 7.98–8.01 (1H, t, J = 8 Hz, Ar–H), 7.82–7.87 (1H, m, Ar–H), 7.75–7.79 (1H, m, Ar–H), 7.65–7.70 (2H, m, Ar–H), 7.41–7.46 (2H, t, J = 8 Hz, Ar–H), 7.11–7.20 (5H, m, Ar–H), 4.84–4.95 (1H, m, CH), 4.70–4.75 (1H, m, CH), 4.17–4.34 (2H, m, CH_2), 3.48–3.60 (2H, m, CH_2), 3.07–3.20 (2H, m, CH_2), 2.23–2.32 (2H, m, CH_2), 1.89–2.15 (2H, m, CH_2), 1.77–1.85 (2H, m, CH_2); ^{13}C NMR (DMSO-D_6, 100 MHz): δ ppm 170.0, 169.6, 158.7, 157.5, 156.8, 156.2, 143.7, 136.9, 135.8, 133.1, 130.6, 128.4, 124.2, 119.5, 97.7, 57.4, 52.2, 46.5, 30.0, 29.5, 29.0, 25.4 & 22.8; IR (KBr disc, cm^{-1}): 3468 s (N–H), 2948 s (sp^2 stretch), 2870 s (sp^3 stretch), 1629 s (C=O stretch), 1567 s (N–H bend), 1490 s, 1441 m (C–H bend), 1312 m (C–F stretch), 1236 s (C–N stretch), 1135 w (C–O stretch), 853 w (N–H oop); HRMS: calcd for $[C_{35}H_{31}BrF_3N_7O_3]^+$ 734.5782, found 734.1652 $[M]^+$ and 756.1491 $[M + Na]^+$.

*1-(2-((R)-3-(4-Amino-3-(4-phenoxyphenyl)-1H-pyrazolo[3,4-d] pyrimidin-1-yl)piperidine-1-carbonyl)pyrrolidin-1-yl)-2-(4-fluorophenyl)ethanone (**12n**).*

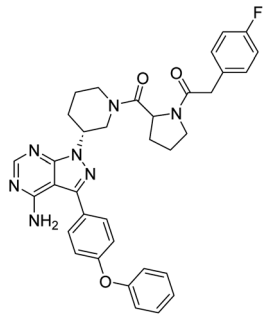

White powder; yield: 361.2 mg (94%); M.P.: 132 °C; ^{1}H NMR (DMSO-D_6, 400 MHz): δ ppm 8.23–8.32 (1H, m, Ar–H), 7.91–8.06 (1H, m, Ar–H), 7.62–7.67 (2H, m, Ar–H), 7.42–7.46 (1H, t, J = 8 Hz, Ar–H), 7.24–7.34 (2H, m, Ar–H), 7.11–7.21 (6H, m, Ar–H), 6.98–7.07 (1H, m, Ar–H), 4.66–4.76 (1H, m, CH), 4.27–4.37 (1H, m, CH), 3.64–3.81 (2H, m, CH_2), 3.52–3.56 (2H, m, CH_2), 3.36–3.37 (2H, m, CH_2), 2.26 (2H, brs, CH_2), 2.10–2.13 (2H, m, CH_2), 1.91–1.97 (2H, m, CH_2), 1.76–1.80 (2H, m, CH_2), 1.30–1.35 (2H, m, CH_2); ^{13}C NMR (DMSO-D_6, 100 MHz): δ ppm 170.5, 168.6, 157.6, 156.8, 155.4, 154.1, 143.9, 136.8, 135.5, 134.2, 132.2, 131.6, 130.8, 130.6, 129.2, 127.1, 126.5, 124.3, 119.4, 115.4, 97.7, 70.4, 60.0, 56.6, 52.3, 47.5, 34.8, 32.0, 22.6, 18.4 & 14.4; IR (KBr disc, cm^{-1}): 3468 s, 3326 s (N–H), 2924 s (sp^2 stretch), 2855 s s (sp^3 stretch), 1639 s (C=O stretch), 1575 s (N–H bend), 1517 m, 1450 s (C–H bend), 1233 s (C–N stretch), 1164 w (C–O stretch), 871 w (N–H oop); HRMS: $[M + H]^+$ calcd for $[C_{35}H_{34}FN_7O_3]^+$ 619.7014, found 620.38 $[M + H]^+$.

*4-Amino-1-((3R)-1-((3-methylbenzoyl)prolyl)piperidin-3-yl)-3-(4-phenoxyphenyl)-1H-pyrazolo[3,4-d]pyrimidine (**12o**).*

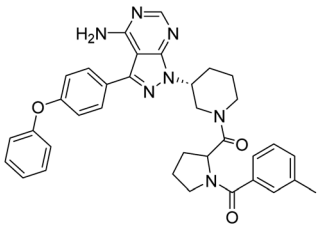

Yellow powder; yield: 302.2 mg (81%); M.P.: 144 °C; ^{1}H NMR (DMSO-D_6, 400 MHz): δ ppm 8.17–8.30 (1H, m, Ar–H), 7.64–7.68 (2H, t, J = 8 Hz, Ar–H), 7.41–7.45 (2H, t, J = 8 Hz, Ar–H), 7.28–7.31 (3H, t, J = 8 Hz, Ar–H), 7.11–7.16 (6H, m, Ar–H), 4.93–5.03 (1H, m, CH), 4.75 (1H, brs, CH), 4.02–4.35 (2H, m, CH_2), 3.40–3.58 (2H, m, CH_2), 2.41–2.43 (2H, m, CH_2), 2.27–2.35 (4H, m, CH_2), 1.87–1.90 (2H, m, CH_2), 1.76 (2H, brs, CH_2), 1.23 (3H, s, CH_3); ^{13}C NMR (DMSO-D_6, 100 MHz): δ ppm 158.7, 157.6, 156.8, 156.1, 154.4, 138.0, 130.6, 128.5, 128.0, 124.2, 119.4, 56.9, 52.3, 50.1, 30.1, 29.4, 29.0, 22.7 & 21.3; IR (KBr disc, cm^{-1}): 3480 s, 3304 s (N–H), 2922 s (sp^2 stretch), 2855 s (sp^3 stretch), 1623 s (C=O stretch), 1568 s (N–H bend), 1521 m, 1480 s, 1438 w (C–H bend), 1222 s (C–N stretch), 1166 w (C–O stretch), 859 w (N–H oop); HRMS: calcd for $[C_{35}H_{35}N_7O_3]^+$ 601.7110, found 602.2846 $[M + 1]^+$, 624.2673 $[M + 1 + Na]^+$ and 626.2737 $[M + 3 + Na]^+$.

*4-Amino-1-((3R)-1-((5-chlorothiophene-2-carbonyl)prolyl)piperidin-3-yl)-3-(4-phenoxyphenyl)-1H-pyrazolo[3,4-d]pyrimidine (**12p**).*

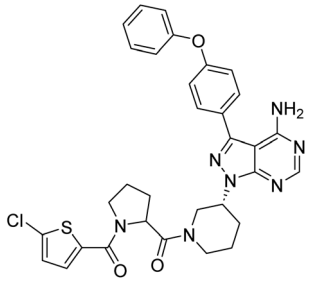

Cream white powder; yield: 307.7 mg (79%); M.P.: 147 °C; ^{1}H NMR (DMSO-D$_6$, 400 MHz): δ ppm 8.24–8.28 (1H, m, Ar–H), 7.67 (2H, brs, Ar–H), 7.54 (1H, brs, Ar–H), 7.44 (2H, brs, Ar–H), 7.15 (6H, brs, Ar–H), 4.94–5.05 (1H, m, CH), 4.70 (1H, brs, CH), 4.31 (2H, brs, CH$_2$), 3.82–3.98 (2H, m, CH$_2$), 3.55 (2H, brs, CH$_2$), 2.15–2.27(2H, m, CH$_2$), 1.87–1.97 (4H, m, CH$_2$), 1.56 (2H, brs, CH$_2$), 1.23 (2H, brs, CH$_2$), 0.84–0.94 (2H, m, CH$_2$); ^{13}C NMR (DMSO-D$_6$, 100 MHz): δ ppm 170.0, 169.6, 159.0, 157.5, 156.8, 156.1, 154.3, 139.5, 130.6, 128.5, 124.2, 119.5, 58.6, 52.2, 49.3, 31.4, 30.0, 28.4, 25.4, 22.5 & 14.4; IR (KBr disc, cm^{-1}): 3468 s, 3309 s (N–H), 2948 s (sp^2 stretch), 2868 s (sp^3 stretch), 1613 s (C=O stretch), 1588 s (N–H bend), 1521 m, 1489 s, 1437 w (C–H bend), 1231 s (C–N stretch), 1166 w (C–O stretch), 846 w (N–H oop); HRMS: calcd for $[C_{32}H_{30}ClN_7O_3S]^+$ 628.1480, found 628.1876 $[M]^+$, 629.1919 $[M + 1]^+$ and 630.1845 $[M + 2]^+$.

*4-Amino-1-((3R)-1-((4-methoxybenzoyl)prolyl)piperidin-3-yl)-3-(4-phenoxyphenyl)-1H-pyrazolo[3,4-d]pyrimidine (**12q**).*

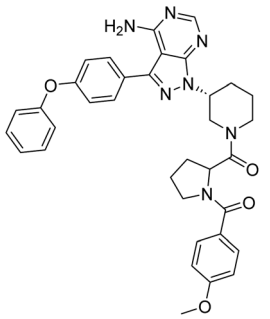

White powder; yield: 307.7 mg (83%); M.P.: 153 °C; ^{1}H NMR (DMSO-D$_6$, 400 MHz): δ ppm 8.23–8.34 (1H, m, Ar–H), 7.67–7.68 (2H, m, Ar–H), 7.42–7.55 (4H, m, Ar–H), 7.12–7.17 (6H, m, Ar–H), 6.98–7.00 (1H, t, J = 8 Hz, Ar–H), 4.92–5.02 (1H, m, CH), 4.72–4.77 (1H, t, J = 8 Hz, CH), 4.35–4.47 (2H, m, CH$_2$), 3.81 (3H, s, OCH$_3$), 3.54 (2H, brs, CH$_2$), 3.29–3.32 (2H, m, CH$_2$), 2.26 (2H, brs, CH$_2$), 2.05–2.16 (2H, m, CH$_2$), 1.89–1.91 (2H, m, CH$_2$), 1.77 (2H, brs, CH$_2$); ^{13}C NMR (DMSO-D$_6$, 100 MHz): δ ppm 160.9, 158.7, 157.6, 156.8, 156.1, 154.4, 130.6, 129.6, 129.2, 128.8, 128.4, 124.2, 119.5, 113.9, 57.1, 55.7, 50.3, 46.5, 30.1, 29.4, 29.0 & 25.6; IR (KBr disc, cm^{-1}): 3466 s, 3397 s (N–H), 2925 s (sp^2 stretch), 2855 s (sp^3 stretch), 1623 s (C=O stretch), 1587 s (N–H bend), 1523 m, 1489 s, 1425 w (C–H bend), 1235 s (C–N stretch), 1167 w (C–O stretch), 871 w (N–H oop); HRMS: calcd for $[C_{35}H_{35}N_7O_4]^+$ 617.7100, found 618.2807 $[M]^+$, 619.2835 $[M + 1]^+$ and 620.2804 $[M + 2]^+$.

*7-Amino-3-((3R)-1-((3-chlorobenzoyl)prolyl)piperidin-3-yl)-1-(4-phenoxyphenyl)-1H-pyrazolo[4,3-d]pyrimidine (**12r**).*

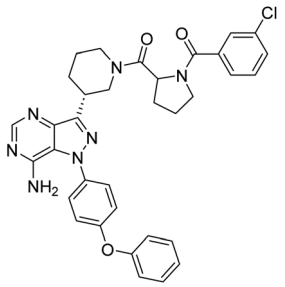

White powder; yield: 327.8 mg (85%); M.P.: 152 °C; ^{1}H NMR (DMSO-D$_6$, 400 MHz): δ ppm 8.24–8.31 (1H, m, Ar–H), 7.63–7.70 (2H, m, Ar–H), 7.54–7.58 (1H, m, Ar–H), 7.49–7.51 (1H, m, Ar–H), 7.40–7.46 (3H, m, Ar–H), 7.33 (1H, brs, Ar–H), 7.11–7.21 (5H, m, Ar–H), 4.91–5.03 (1H, m, CH), 4.71–4.83 (1H, m, CH), 4.01–4.35 (2H, m, CH$_2$), 3.56–3.63 (2H, m, CH$_2$), 3.28–3.30 (2H, m, CH$_2$), 2.11–2.33 (2H, m, CH$_2$), 1.91–2.02 (4H, m, CH$_2$), 1.73–1.80 (2H, m, CH$_2$); ^{13}C NMR (DMSO-D$_6$, 100 MHz): δ ppm 172.5, 170.5, 168.0, 166.6, 158.7, 157.5, 156.2, 143.7, 140.1, 133.5, 130.6, 129.8, 127.2, 126.1, 124.2, 119.4, 97.8, 59.6, 57.2, 52.2, 31.4, 30.5, 25.4, 22.5, 21.5 & 14.5; IR (KBr disc, cm^{-1}): 3481 s, 3196 s (N–H), 2924 s (sp^2 stretch), 2857 s (sp^3 stretch), 1625 s (C=O stretch), 1567 s (N–H bend), 1480 s, 1439 w (C–H bend), 1221 s (C–N stretch), 1141 w (C–O stretch), 859 w (N–H oop), 762 w (C–Cl stretch); HRMS: calcd for $[C_{34}H_{32}ClN_7O_3]^+$ 622.1260, found 622.2317 $[M]^+$, 623.2348 $[M + 1]^+$ and 624.2323 $[M + 2]^+$, 644.2138 $[M + Na]^+$, 644.2125 $[M + Na + 1]^+$, 648.2165 $[M + Na + 2]^+$.

*7-Amino-3-((3R)-1-((4-nitrobenzoyl)prolyl)piperidin-3-yl)-1-(4-phenoxyphenyl)-1H-pyrazolo[4,3-d]pyrimidine (**12s**).*

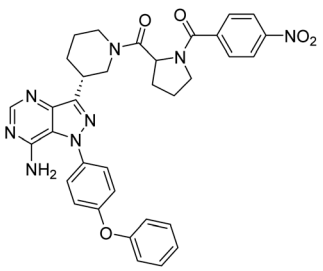

Yellowish-white powder; yield: 337.3 mg (86%); M.P.: 155 °C; ^{1}H NMR (DMSO-D$_6$, 400 MHz): δ ppm 8.42–8.44 (1H, d, J = 8 Hz, Ar–H), 8.29–8.37 (1H, m, Ar–H), 7.78–7.84 (1H, m, Ar–H), 7.67–7.73 (3H, m, Ar–H), 7.46–7.48 (2H, m, Ar–H), 7.16–7.23 (5H, m, Ar–H), 4.97–5.11 (1H, m, CH), 4.79–4.81 (1H, m, CH), 3.91–4.52 (2H, m, CH$_2$), 3.66–3.68 (2H, m, CH$_2$), 3.46–3.48 (2H, m, CH$_2$), 2.21–2.38 (2H, m, CH$_2$), 2.05–2.07 (2H, m, CH$_2$), 1.80–1.86 (2H, m, CH$_2$); ^{13}C NMR (DMSO-D$_6$, 100 MHz): δ ppm 170.0, 168.1, 166.4, 158.7, 157.5, 156.8, 156.1, 154.3, 148.3, 143.8, 130.6, 128.9, 128.3, 124.1, 119.5, 97.7, 59.3, 52.2, 36.2, 31.3, 29.5, 25.3, 23.0, 21.6 & 14.4; IR (KBr disc, cm^{-1}): 3468 s, 3317 s (N–H), 2925 s (sp^2 stretch), 2856 s (sp^3 stretch), 1631 s (C=O stretch),

1596 s (N–H bend), 1522 m, 1488 s, 1436 w (C–H bend), 1346 s (N–O stretch), 1235 s (C–N stretch), 1103 w (C–O stretch), 867 w (N–H oop); HRMS: calcd for $[C_{34}H_{32}N_8O_5]^+$ 632.6810, found 633.1482 $[M]^+$, 634.1482 $[M + 1]^+$ and 635.1465 $[M + 2]^+$.

*((R)-3-(7-Amino-1-(4-phenoxyphenyl)-1H-pyrazolo[4,3-d] pyrimidin-3-yl)piperidin-1-yl)(1-(5-((6-chloro-2-methylpyrimidin-4-yl)amino)thiazole-2-carbonyl)pyrrolidin-2-yl)methanone (**12t**).*

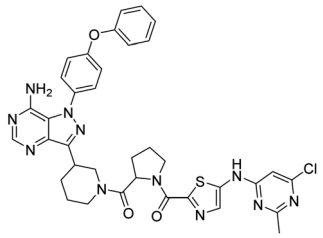

White powder; yield: 419.96 mg (92%); M.P.: 278 °C; ^{1}H NMR (DMSO-D_6): δ ppm ^{1}H NMR (DMSO-D_6, 400 MHz): δ ppm 8.24–8.29 (1H, m, Ar–H), 7.98–8.01 (1H, d, $J = 12$ Hz, Ar–H), 7.60–7.68 (2H, m, Ar–H), 7.42–7.46 (2H, t, $J = 4$ Hz, Ar–H), 7.15–7.21 (5H, m, Ar–H), 6.94 (1H, brs, Ar–H), 5.06 (1H, m, CH), 4.71–4.72 (1H, m, CH), 4.33–4.39 (2H, m, CH_2), 3.84–3.86 (2H, m, CH_2), 3.57–3.63 (2H, m, CH_2), 2.60 (3H, s, CH_3), 2.18–2.30 (4H, m, CH_2), 1.81–1.98 (4H, m, CH_2); ^{13}C NMR (DMSO-D_6, 100 MHz): δ ppm 170.3, 167.9, 161.3, 160.1, 158.7, 157.5, 156.8, 156.1, 154.3, 143.7, 141.0, 130.6, 128.9, 124.2, 119.5, 103.9, 97.7, 58.3, 52.3, 49.1, 46.5, 45.7, 30.1, 28.5, 26.8 & 25.7; IR (KBr disc, cm^{-1}): 3470 s (N–H), 2924 s (sp^2 stretch), 2851 s (sp^3 stretch), 1574 s (C═O stretch, N–H bend), 1523 s, 1489 s, 1408 w (C–H bend), 1238 s (C–N stretch), 1129 w (C–O stretch), 850 w (N–H oop); ESI-MS: calcd for $[C_{36}H_{34}ClN_{11}O_3S]^+$ 736.2520, found 736.23 $[M]^+$, and 737.22 $[M + 1]^+$.

Biological studies

Based on their structural novelty, all synthesized compounds were tested for a preliminary single-dose screening under the Developmental Therapeutics Program by the National Cancer Institute, USA. A one-dose screening was performed at a single high dose of 10 μM for all synthesized compounds across all cell lines in the NCI60 panel consisting of 60 human tumour cell lines from nine tissue origins: leukaemia, breast, lung, prostate, renal, ovarian, melanoma, central nervous system, and colon. Following this, only the compounds that exhibited exceptional activity in a maximum number of tumour cell lines were taken up for a dose-dependent experiment to understand the anti-cancer efficacy of the compounds.

Sulforhodamine B (SRB) colorimetric assay was performed as per the literature,[33] in both single and five-dose assays, to evaluate the *in vitro* effectiveness of the compounds. Shortly, the tumour cell lines were cultures in RPMI 1640 medium containing 5% fetal bovine serum and 2 mM l-glutamine. The plating densities for the cells in 96 well plates ranged from 5000 to 40 000 cells per well depending on the doubling time of individual cell lines. The well plates were incubated at 37 °C, 5% CO_2, 95% air and 100% relative humidity for 24 h before adding experimental drugs. The compounds were solubilized in DMSO. For the five-dose experiment, the compounds were diluted by $\frac{1}{2}$ log serial dilutions to provide five different concentrations (*i.e.*, −8 to −4 log concentrations or 100 to 0.01 μM) along with control. The plates were incubated for 48 hours before the addition of SRB solution at 0.4% (w/v) in 1% acetic acid (100 μL per well), incubated for another 10 minutes before the bound stain was stained with 10 mM Trizma base, and the absorbance is read on an automated plate reader at 515 nm. The half maximal effective concentration (IC_{50}) was calculated from $[(T_i - T_z)/(C - T_z)] \times 100 = 50$, which is the drug concentration resulting in a 50% reduction in the net protein increase (as measured by SRB staining) in control cells during the drug incubation, where T_i = test growth in presence of the drug agent, T_z = absorbance at time zero, and C = control growth. All experiments were conducted in triplicates and the man values were represented in this paper. A detailed description of the screening process and methodology is available at the DTP website (**https://dtp.cancer.gov/discovery_development/nci-60/methodology.htm**).

Conclusions

In this study, we successfully synthesized and characterized a novel library of 20 compounds featuring a 4-aminopyrazolo [3,4-*d*]pyrimidine core using advanced spectroscopic techniques. These compounds were evaluated for their growth inhibitory activities against 60 human tumor cell lines across nine cancer panels, demonstrating significant anticancer activity, particularly in leukemia, melanoma, and renal cancer cell lines. Compounds **11**, **12c**, **12d**, **12f**, and **12j** especially stood out with superior activity compared to established small molecule drugs. Compound **12c** demonstrated 2.88 times greater activity than sorafenib and 1.45 times greater than sunitinib when tested against the UO-31 renal cancer cell line. Structure–activity relationship analysis provided insights into the critical structural features influencing biological activity, and several compounds exhibited *in vitro* activity comparable to or exceeding that of known small molecule therapies. These findings underscore the potential behavior of 4-aminopyrazolo[3,4-*d*]pyrimidine derivatives as promising candidates as anti-cancer molecules for further development, warranting additional preclinical studies to fully elucidate their therapeutic potential and mechanisms of action.

Data availability

All the analyzed data during this work was included in the published article.

Author contributions

AD and GV conceived and designed the analysis. MBH and MSA drafted the manuscript, and PKG and MN analyzed the data and edited the manuscript. All authors read and approved the final manuscript.

Conflicts of interest

There are no conflicts to declare.

Acknowledgements

The authors sincerely thank SVAK Life Science, Hyderabad, for their invaluable support and encouragement throughout this study. Special thanks are also extended to the Central Research Laboratory (CRL) and the Central Research Instrumental Facility (CRIF) at SSSIHL, Andhra Pradesh, for providing access to essential resources and advanced instrumentation, which were crucial for the successful completion of this research. The PI wishes to thank the National Cancer Institute, Developmental Therapeutics Program (NCI/DTP), https://dtp.cancer.gov for providing screening data of compounds.

References

1 Cancer (IARC) TIA for R on Global Cancer Observatory, accessed April 30, 2024, https://gco.iarc.fr/.

2 Global cancer burden growing, amidst mounting need for services, accessed April 30, 2024, https://www.who.int/news/item/01-02-2024-global-cancer-burden-growing–amidst-mounting-need-for-services.

3 M. Albratty and H. A. Alhazmi, Novel pyridine and pyrimidine derivatives as promising anticancer agents: A review, *Arabian J. Chem.*, 2022, **15**(6), 103846, DOI: 10.1016/j.arabjc.2022.103846.

4 R. S. Mohana and R. Sompalle, Synthetic chemistry of pyrimidines and fused pyrimidines: A review, *Synth. Commun.*, 2016, **46**(8), 645–672, DOI: 10.1080/00397911.2016.1165254.

5 S. A. Benner, Understanding Nucleic Acids Using Synthetic Chemistry, *Acc. Chem. Res.*, 2004, **37**(10), 784–797, DOI: 10.1021/ar040004z.

6 R. J. Thomson, M. Moshirfar and Y. Ronquillo. Tyrosine Kinase Inhibitors, in *StatPearls*, StatPearls Publishing, 2023, accessed December 7, 2023, http://www.ncbi.nlm.nih.gov/books/NBK563322/.

7 J. T. Hartmann, M. Haap, H. G. Kopp and H. P. Lipp, Tyrosine kinase inhibitors - a review on pharmacology, metabolism and side effects, *Curr. Drug Metab.*, 2009, **10**(5), 470–481, DOI: 10.2174/138920009788897975.

8 M. A. Carrato, E. Grande Pulido and C. Guillén-Ponce, Understanding the molecular-based mechanism of action of the tyrosine kinase inhibitor: sunitinib, *Anti-Cancer Drugs*, 2010, **21**, S3, DOI: 10.1097/01.cad.0000361534.44052.c5.

9 R. J. Spandl, M. Díaz-Gavilán, K. M. G. O'Connell, G. L. Thomas and D. R. Spring, Diversity-oriented synthesis, *Chem. Rec.*, 2008, **8**(3), 129–142, DOI: 10.1002/tcr.20144.

10 W. R. J. D. Galloway, A. Isidro-Llobet and D. R. Spring, Diversity-oriented synthesis as a tool for the discovery of novel biologically active small molecules, *Nat. Commun.*, 2010, **1**(1), 80, DOI: 10.1038/ncomms1081.

11 L. Hudson, J. W. Mason, M. V. Westphal, *et al.*, Diversity-oriented synthesis encoded by deoxyoligonucleotides, *Nat. Commun.*, 2023, **14**(1), 4930, DOI: 10.1038/s41467-023-40575-5.

12 A. Dash, G. Vaddamanu, R. Karreddula, S. S. B. Manubolu, P. G. Kumari and N. Mulakayala, Novel N-(3-ethynyl Phenyl)-6,7-bis(2-methoxyethoxy)Quinazoline-4-amine Derivatives: Synthesis, Characterization, Anti-cancer Activity, In-silico and DFT Studies, *Anti-Cancer Agents Med. Chem.*, 2024, **24**(7), 514–532, DOI: 10.2174/0118715206276286231220055233.

13 O. D. Abaan, E. C. Polley, S. R. Davis, *et al.*, The exomes of the NCI-60 panel: a genomic resource for cancer biology and systems pharmacology, *Cancer Res.*, 2013, **73**(14), 4372–4382, DOI: 10.1158/0008-5472.CAN-12-3342.

14 (*a*) S. Shafi, M. M. Alam, N. Mulakayala, C. Mulakayala, G. Vanaja, A. M. Kalle, R. Pallu and M. S. Alam, Synthesis of novel 2-mercapto benzothiazole and 1,2,3-triazole based bis-heterocycles: their anti-inflammatory and anti-nociceptive activities, *Eur. J. Med. Chem.*, 2012, **49**, 324–333; (*b*) N. Mulakayala, P. Rao, J. Iqbal, R. Bandichhor and S. Oruganti, Synthesis of novel therapeutic agents for the treatment of multiple sclerosis: a brief overview, *Eur. J. Med. Chem.*, 2013, **60**, 170–186; (*c*) H. Sudhakar, G. Pavana Kumari and N. Mulakayala, Montmorillonite K10 as highly efficient catalyst for the synthesis of phenols from arylboronic acids, *Ind. J Adv. Chem. Sci.*, 2013, **13**(2), 57–61; (*d*) H. Sudhakar, G. Pavana Kumari, R. Venkata Nadh and N. Mulakayala, Green approach toward the synthesis of n-substituted anilines via smile rearrangement using amberlite IR-400 resin, *Ind. J Adv. Chem. Sci.*, 2014, **2**, 294–299; (*e*) K. B. Ismail, G. Thalari, V. Bommarapu, C. Mulakayala, S. K. Chita and N. Mulakayala, Synthesis of novel spiro[pyrazolo[4,3-d]pyrimidinones and spiro[benzo[4,5]thieno[2,3-d]pyrimidine-2,3′-indoline]-2′,4(3H)-diones and their evaluation for anticancer activity, *Bioorg. Med. Chem. Lett.*, 2017, **27**, 1446–1450; (*f*) N. Mulakayala, B. Kandagatla, R. R. K. Ismail, P. Rao, C. Mulakayala, C. S. Kumar, J. Iqbal and S. Oruganti, Synthesis of novel spiro[pyrazolo[4,3-d]pyrimidinones and spiro[benzo[4,5]thieno[2,3-d]pyrimidine-2,3′-indoline]-2′,4(3H)-diones and their evaluation for InCl3-catalysed synthesis of 2-aryl quinazolin-4 (3H)-ones and 5-aryl pyrazolo [4, 3-d] pyrimidin-7 (6H)-ones and their evaluation as potential anticancer agents, *Bioorg. Med. Chem. Lett.*, 2012, **15**, 5063–5066; (*g*) N. Mulakayala, D. Rambabu, M. R. Raja, M. Chaitanya, C. S. Kumar, A. M. Kalle, G. R. Krishna, C. M. Reddy, M. V. B. Rao and M. Pal, Ultrasound mediated catalyst free synthesis of 6H-1-benzopyrano [4, 3-b] quinolin-6-ones leading to novel quinoline derivatives: Their evaluation as potential anti-cancer agents, *Bioorg. Med. Chem.*, 2012, **20**, 759–768.

15 H. Willitzer, M. Tonew and E. Lippmann, Considerations on Structure-Activity Relationships with Mengovirus of Substituted 5-Amino-4-Cyanopyrazoles, *Antimicrob. Agents Chemother.*, 1976, **9**(3), 367–370, DOI: 10.1128/aac.9.3.367.

16 L. Dee Nord, R. C. Willis, D. F. Smee, T. A. Riley, G. R. Revankar and R. K. Robins, Inhibition of orotidylate decarboxylase by 4(5H)-oxo-1-β-d-ribofuranosylpyrazolo[3,4-d] pyrimidine-3-thiocarboxamide (APR-TC) in B lymphoblasts: Activation by adenosine kinase, *Biochem. Pharmacol.*, 1988, **37**(24), 4697–4705, DOI: **10.1016/0006-2952(88)90340-1**.

17 D. G. Johns, Metabolism of Cancer Chemotherapeutic Agents via Pathways Utilized by Endogenous Substrates, in *Antineoplastic and Immunosuppressive Agents Part I. Handbuch der experimentellen Pharmakologie/Handbook of Experimental Pharmacology*, ed. Sartorelli A. C. and Johns D. G., Springer, 1974, pp. 270–287, DOI: **10.1007/978-3-642-65678-1_14**.

18 M. H. Elnagdi, M. R. H. El-Moghayar, D. H. Fleita, E. A. A. Hafez and S. M. Fahmy, Pyrimidine derivatives and related compounds. 4. A route for the synthesis of pyrazolo[3,4-e]-as-triazines, pyrazolo[3,4-d]pyrimidines, and pyrazolo[1,5-c]-as-triazines, *J. Org. Chem.*, 1976, **41**(24), 3781–3784, DOI: **10.1021/jo00886a002**.

19 B. Paul, M. F. Chen and A. R. P. Paterson, *Inhibitors of Nucleoside Transport. Structure-Activity Study Using Human Erythrocytes*, ACS Publications, DOI: **10.1021/jm00244a003**.

20 K. R. Cousins, ChemDraw Ultra 9.0. CambridgeSoft, 100 CambridgePark Drive, Cambridge, MA 02140. www.cambridgesoft.com. See Web site for pricing options, *J. Am. Chem. Soc.*, 2005, **127**(11), 4115–4116, DOI: **10.1021/ja0410237**.

21 N. M. O'Boyle, M. Banck, C. A. James, C. Morley, T. Vandermeersch and G. R. Hutchison, Open Babel: An open chemical toolbox, *J. Cheminf.*, 2011, **3**(1), 33, DOI: **10.1186/1758-2946-3-33**.

22 P. Skehan, R. Storeng, D. Scudiero, *et al.*, New Colorimetric Cytotoxicity Assay for Anticancer-Drug Screening, *JNCI, J. Natl. Cancer Inst.*, 1990, **82**(13), 1107–1112, DOI: **10.1093/jnci/82.13.1107**.

23 P. Chen, N. V. Lee, W. Hu, *et al.*, Spectrum and Degree of CDK Drug Interactions Predicts Clinical Performance, *Mol. Cancer Ther.*, 2016, **15**(10), 2273–2281, DOI: **10.1158/1535-7163.MCT-16-0300**.

24 A. Lebedevs, J. Ponomarjovs, L. Varaceva, D. Cernaks, A. Cernobrovijs and E. Lavrinovics, A method for preparation of ibrutinib precursor, Published online March 9, 2017, accessed January 13, 2024. **https://patents.google.com/patent/WO2017039425A1/en**.

25 A. K. Ghosh and D. Shahabi, Synthesis of amide derivatives for electron deficient amines and functionalized carboxylic acids using EDC and DMAP and a catalytic amount of HOBt as the coupling reagents, *Tetrahedron Lett.*, 2021, **63**, 152719, DOI: **10.1016/j.tetlet.2020.152719**.

26 C. A. G. N. Montalbetti and V. Falque, Amide bond formation and peptide coupling, *Tetrahedron*, 2005, **61**(46), 10827–10852, DOI: **10.1016/j.tet.2005.08.031**.

27 A. Kumar, H. K. Akula and M. K. Lakshman, Simple Synthesis of Amides and Weinreb Amides via Use of PPh3 or Polymer-Supported PPh3 and Iodine, *Eur. J. Org. Chem.*, 2010, **2010**(14), DOI: **10.1002/ejoc.200901420**.

28 E. Sturabotti, F. Vetica, G. Toscano, *et al.*, N-Acetyl-l-phenylalanine Racemization during TBTU Amidation: An In-Depth Study for the Synthesis of Anti-Inflammatory 2-(N-Acetyl)-l-phenylalanylamido-2-deoxy-d-glucose (NAPA), *Molecules*, 2023, **28**(2), 581, DOI: **10.3390/molecules28020581**.

29 O. N. Ikediobi, H. Davies, G. Bignell, *et al.*, Mutation analysis of 24 known cancer genes in the NCI-60 cell line set, *Mol. Cancer Ther.*, 2006, **5**(11), 2606–2612, DOI: **10.1158/1535-7163.MCT-06-0433**.

30 A. M. Gholami, H. Hahne, Z. Wu, *et al.*, Global Proteome Analysis of the NCI-60 Cell Line Panel, *Cell Rep.*, 2013, **4**(3), 609–620, DOI: **10.1016/j.celrep.2013.07.018**.

31 Molecular Characterization of the NCI-60 | NCI-60 Human Tumor Cell Lines Screen | Discovery & Development Services | Developmental Therapeutics Program (DTP), accessed January 13, 2024, **https://dtp.cancer.gov/discovery_development/nci-60/characterization.htm**.

32 D. L. Hughes, Patent Review of Manufacturing Routes to Recently Approved Oncology Drugs: Ibrutinib, Cobimetinib, and Alectinib, *Org. Process Res. Dev.*, 2016, **20**(11), 1855–1869, DOI: **10.1021/acs.oprd.6b00304**.

33 E. A. Orellana and A. L. Kasinski, Sulforhodamine B (SRB) Assay in Cell Culture to Investigate Cell Proliferation, *Bio-Protoc.*, 2016, **6**(21), e1984, DOI: **10.21769/BioProtoc.1984**.